Unified Rate Theory of Electrochemistry and Electrocatalysis: Fixed Potential Formulation for General, Electron Transfer, and Proton-Coupled Electron Transfer Reactions

Marko M. Melander

Nanoscience Center, P.O. Box 35 (YN) FI-40014, Department of Chemistry, University of Jyväskylä, Finland

Abstract

Atomistic modeling of electrocatalytic reactions is most naturally conducted within the grand canonical ensemble (GCE) which enables fixed chemical potential calculations. While GCE has been widely adopted for modeling electrochemical and electrocatalytic thermodynamics, the electrochemical reaction rate theory within GCE is lacking. Molecular and condensed phase rate theories are formulated within microcanonical and canonical ensembles, respectively, but electrocatalytic systems described within the GCE require extension of the conventionally used rate theories for computation reaction rates at fixed electrode potentials. In this work, rate theories from (micro)canonical ensemble are generalized to the GCE providing the theoretical basis for the computation reaction rates in electrochemical and electrocatalytic systems. It is shown that all canonical rate theories can be extended to the GCE. From the generalized grand canonical rate theory developed herein, fixed electrode potential rate equations are derived for i) general reactions within the GCE transition state theory (GCE-TST), ii) adiabatic curve-crossing rate theory within the empirical valence bond theory (GCE-EVB), and iii) (non-)adiabatic electron and proton-coupled electron transfer reactions. The rate expressions can be readily combined with *ab initio* methods to study reaction kinetics reactions at complex electrochemical interfaces

Email address: marko.m.melander@jyu.fi (Marko M. Melander)

as a function of the electrode potential. The theoretical work herein provides a single, unified approach for electrochemical and electrocatalytic kinetics and the inclusion of non-adiabatic and tunneling effects in electrochemical environments widening the scope of reactions amenable to computational studies.

Keywords: charge transfer, Tafel slope, electrochemical kinetics, Marcus theory, grand canonical

1. Introduction

Electrochemical reactions and especially electrocatalysis are at the forefront of current green technologies. Electrocatalytic conversion of small molecules to fuels, energy and useful chemicals are key components of a sustainable future. To realize and utilize the full potential of electrocatalysis, selective and active catalysts are needed for various applications and reactions including *e.g.* oxygen and hydrogen reduction/evolution reactions, nitrogen reduction to ammonia and CO_2 reduction.[1] Electrochemical conversion of small molecules is most often based on successive proton-coupled electron transfer (PCET), electron transfer (ET), and proton transfer (PT) reactions; the unique aspect of electrocatalysis is the ability to control PCET, ET, and PT kinetics and thermodynamics by the electrode potential.

Tational design of better electrocatalysts working under complex electrochemical environments needs insight from experiments, computational methods as well as theoretical approaches.[1] Experimental techniques have reached certain maturity and tools such as potential sweep and step methods, spectroelectrochemistry, and impedance spectroscopy are standard tools for understanding electrocatalytic reactions.[2] However, a similar level of maturity has not yet been reached within the computational and theoretical electrochemistry communities. Currently, there are several competing but often overlapping computational approaches available for studying reactions at electrochemical interfaces.

Experimentally electrocatalysis is controlled by the electrolyte and electrode potential. To translate these to computationally treatable quantities, it is the combination of the electrolyte and electron electrochemical potentials which determine and control the (thermodynamic) state of electrochemical systems. Therefore, an atomic-level computational model needs to provide an explicit control and description of these chemical potentials as depicted

in Figure 1. In statistical thermodynamics fixing the chemical potentials is achieved *via* a Legendre transformation from a canonical ensemble to a grand-canonical ensemble (GCE) for both electrons and nuclei[3] Then, chemical potentials are fixed while particle numbers are allowed to fluctuate.

This calls for theoretical and computational approaches within the grand-canonical ensemble (GCE) in which chemical potentials are fixed while particle numbers are allowed to fluctuate. In electronic structure calculations as applied to electrochemical systems one of the largest difficulties is indeed modelling systems at constant electrode potentials rather than constant charges; this corresponds to a change from a fixed particle canonical ensemble to an open, fixed (electro)chemical potential ensemble. This is a rather drastic difference and almost all electronic structure codes work exclusively for fixed charge calculations. Another difficulty faced in simulating electrochemistry is the presence of several time- and length-scales taking part in the processes. Very short time and small length-scales are needed when modelling charge transfer and chemical reactions which call for a quantum mechanical treatment of the electrode and reactants. On the other hand, the liquid electrolyte and formation of the electrochemical double-layer need a statistical treatment over a long time to properly represent the electrified solid-liquid interface. The charge distribution at the interface is controlled by the electrode potential which also directly changes both reaction kinetics and thermodynamics.

The theoretical basis for fixed potential electronic structure calculations was developed by Mermin who formulated electronic density functional theory (DFT) within GCE.[4, 5]. Later, the GCE-DFT has been generalized to treat nuclear species both classically or quantum mechanically [3, 6–9]. The GCE-DFT provides a fully DFT, atomistic approach for computing free energies of electrochemical and electrocatalytic systems at fixed electrode and ionic/nuclear chemical potentials.[3] Importantly, the free energy from a GCE-DFT calculation is in theory exact and unique to a given external potential. In practice, the (exchange-)correlation effects in both quantum and classical systems need to be approximated.

Atom-scale modeling of electrocatalytic reactions at fixed electrode[3, 10–20] and ion potentials[3, 12, 14] at electrochemical interfaces has been greatly advanced during the last 10-15 years and utilized in large scale studies of reactions at electrode surfaces. The work in the field of atomistic modelling of electrocatalytic reactions has been on almost exclusively focused on electrocatalytic thermodynamics. Based on the large number of theoretical and

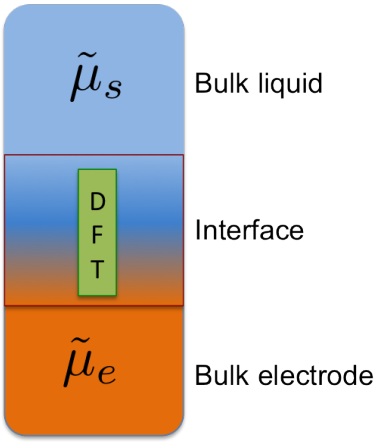

Figure 1: Pictorial model of a proper electrochemical interface at fixed electron $\tilde{\mu}_e$ and solvent/electrolyte $\tilde{\mu}_S$ chemical potentials the atomic level.

computational works utilizing GCE-DFT, the framework for thermodynamics within GCE seems generally accepted.

However, computation of electrochemical kinetics from atomistic simulations has remained more elusive. Like the electrochemical thermodynamics, also the kinetics should be computed at fixed electrochemical potentials. This calls for generalization of fixed particle number canonical rate theories to the fixed potential GCE. Surprisingly, a general GCE rate theory has not yet been established; mending this deficiency is the central goal of the present work. As discussed in detail below, the GCE rate theory must facilitate computation of rate constants for general chemical reactions and especially PCET, ET, and PT at fixed chemical potentials. Furthermore, the theory must be applicable to both inner-sphere and adiabatic as well as outer-sphere, non-adiabatic and tunneling reactions at constant potentials. In fact, the lack of generally applicable kinetic models to treat non-adiabaticity and tunneling in electrocatalytic ET, PT, and PCET under fixed potential situations limits the scope computational and theoretical investigations of reactions to adiabatic inner-sphere reactions - a very limited subset of electrochemical and electrocatalytic reactions. This current restriction is caused by the absence of theoretical and computational methodologies[21]; while thermodynamics and kinetics of simultaneous PCET reactions are easy to evaluate for fully adiabatic inner-sphere reactions using (grand) canonical DFT and (harmonic) transition state theory (TST) *vide infra*, decoupled PCET reactions, outer-sphere ET/PT and non-adiabatic PCET reactions require more

advanced methods.

In general, ET, PT, and PCET reactions may exhibit both vibronic and electronic non-adiabaticity as well as hydrogen tunneling. The importance and contribution of non-adiabaticity and tunneling may also depend on the the electrode potential.[22, 23] There are several reactions where decoupled PCET *i.e.* separate ET and PT steps, hydrogen tunneling and non-adiabaticity have been observed. For example, in alkaline ORR pure ET has been proposed as the rate determining step[21, 24–26]. Furthermore, recent experiments of ORR on carbon-based materials show conclusively that ET is the rate- and potential-determining step.[27, 28]. On the other hand, solution pH can alter the reaction mechanism and *,e.g.,* CO_2 reduction can proceed through simultaneous PCET in acidic and through decoupled PCET (ET-PT) in alkaline solutions[29, 30]. It has also been shown that only the inclusion of vibronic non-adiabaticity in electrochemical hydrogen evolution reaction can explain experimentally observed Tafel slopes and kinetic isotope effects.[22] There is also experimental evidence that room-temperature hydrogen tunneling takes place during ORR Pt and at low over-potentials tunneling is the prevalent reaction pathway.[23] Kinetics of ET are needed to describe both pure ET and decoupled PCET and in general it is expected that these pathways may prevail on weakly bonding electrode surfaces in oxygen, CO_2, CO, alcohol *etc.* reduction reactions.[31] In fact, PCET reactions are often vibronically and/or electronically non-adiabatic[32], even under electrocatalytic conditions[22].

Even though a general GCE rate theory is missing, schemes for computing rates or energy barriers of adiabatic reactions at constant electrode potentials have started to emerge. In some cases reaction barriers have been calculated explicitly at a given electrode potentials using GCE-DFT[12, 20, 33–35]. However, more often various correction schemes to (Legendre) transform constant charge calculations to GCE are used for studying reaction kinetics.[11, 19, 36–39]. From both approaches the grand energy potentials as a function of the electrode potential or along the reaction coordinate are often found to exhibit quadratic dependence. This quadratic dependence of the grand energy as a function of the potential has been used to transform canonical DFT barriers and reaction energies to grand energies. Recently, it has been noticed that reaction barriers as a function of the potential follow a "Marcus-like" [20] or Brønsted-Evans-Polanyi (non)-linear[38] free energy relations. Other approaches for computing electrode potential-dependent barrier have relied on Butler-Volmer -type (BV) expressions where the bar-

rier has a simple form $G(\eta) = G(\eta = 0) + \alpha\eta$ where η is the over-potential and $\alpha \in [0, 1]$ is the BV symmetry factor.[38, 40, 41]. Independent of the scheme used for obtaining a constant potential reaction barrier, TST-like expressions has been used to compute rate without a sound theoretical basis for the validity of GCE-TST.

Even if GCE-TST proved to be valid (as it does based on the work herein), non-adiabatic and tunneling effects in ET, PT, and PCET effects would be omitted in the fully adiabatic treatments with classical nuclei described above. While neglecting these effects may be reasonable for many electrocatalytic reactions, all electrocatalytic reactions are certainly not inner-sphere nor adiabatic as was discussed. A handful computational and theoretical studies[22, 24, 42–48] at the electronic structure level have studied non-adiabaticity or tunneling effects in electrocatalytic ET/PCET. These pioneering studies utilized simplified model Hamiltonians and wave functions and computation of non-adiabatic/tunneling effects in electrocatalytic reactions. However, using general first principles methods for addressing ET/PCET kinetics have remained elusive thus far. Past theoretical and computational work on non-adiabatic electrochemical ET and PCET rates at a given electrode potentials have been accomplished using either Dogonadze-Kutzetnotsov-Levich[49, 50], Schmickler-Newns-Anderson[51, 52], or Soudackov-Hammes-Schiffer[22, 32, 45, 53–55] methods. In these treatments the electrode potential is treated as an external parameter modifying the reaction energy or barrier. These models can also incorporate electrostatic interactions between the electrode and the reactant in the double-layer. When combined with first principles simulations, the electronic structure, orbitals, or density of states are computed once for a fixed number of electrons. Then, the electrode potential serves to role of changing the Fermi-level of this static electronic structure. In such calculations the electronic structure itself is considered unaltered when the potential is changed. While this might be valid in some cases, in general the electrode potential changes the solvent structure, bonding of reactants, double-layer, electronic density of states, overlap integrals *etc.* limiting the applicability of the static picture. Instead, modern fixed potential first-principles methods explicitly incorporate the effect of electrode potentials on the interfacial properties and bonding. Another inherent limitation occurring in previous work addressing non-adiabaticity in ET is the limitation to a single orbital picture. The traditional models assume transitions between different electrode single electron states and redox-levels of the molecule to be independent. Technically, achieving this

requires separating the total wave function to filled/empty and localized orbitals. An inherent problem encountered is that this wave function separation cannot be achieved without additional assumptions as shown in Appendix A. In practice this hampers the computation of ET rates from DFT or wave function methods because an additional (and rather) arbitrary orbital separation/localization step is required.

A general electrocatalytic rate theory should not be restricted to model (single-orbital) wave functions or Hamiltonians. Instead, a many-electron wave function obtained using *ab initio* methods at a fixed potential should be used to capture the inherent complexity reactions at electrochemical interfaces. In the canonical ensemble, ET and PCET rates of electronically and vibronically (non-)adiabatic reactions can be studied using either model or general Hamiltonians[32, 54–60]. Extending these canonical rate theories to fixed potential GCE is the direction pursued herein. This is important from both practical and conceptual point of views that electronic and vibronic non-adiabaticity and tunneling can be included in electrochemical, fixed potential ET, PT and PCET rates using generalized Hamiltonians, many-electron wave functions, and rate theory.

The above discussion highlights that electrochemical (outer-sphere) and electrocatalytic (inner-sphere) reactions have treated using different approaches. Commonly, electrocatalytic reactions have been studied using adiabatic TST theory while electrochemical reactions have relied on perturbative non-adiabatic theories. However, in the canonical ensemble, all rate theories equally applicable to inner- or outer-sphere reactions can be derived using a single general framework provided by Miller[61–63]. This general theory forms the basis of the extension to grand canonical rate theories of the current work.

The importance and impact of the of the general framework in the electrocatalytic context is best appreciated by considering how different rate theories enable description of (electro)catalytic reactions and phenomena. Of course, archetypal adiabatic reactions, including simultaneous adiabatic PCET reactions, can be studied using the common (harmonic) TST with classical nuclei.[61] The real power of the general rate theories is the ability to extend them to treat reactions where tunneling or non-adiabaticity are important. Such methods include ring-polymer TST[64–67], path-integral TST[68], semi-classical instanton methods[67, 69], or semi-classical TST[70, 71], for example. Also non-adiabatic ET and PCET reactions can be modelled within the general framework by using non-adiabatic TST[54, 55, 72–74] which at the classical limit gives a Marcus-type equation[75] for the barrier and a

non-adiabatic correction for the transmission coefficient can be included.

The goal of the present work is to formulate a general rate theory for reactions taking place at fixed (electro)chemical potentials. The formulation is equally applicable to electrocatalytic and electrochemical reactions and, hence, presents a general unified approach. This includes the possibility to account for tunneling as well as vibronic and electronic non-adiabaticity. While methods for treating thermodynamics, locating transition states and energy barriers within GCE have been devised, a general method for computation reaction rates – not just barriers – is not yet available. Here this is obtained by extending general (micro)canonical rate theories to electrochemical systems using a GCE formulation developed herein. The GCE rate theory enables the use of all canonical rate theories in constant potential simulations.

In this work, the general framework is developed and utilized to derive rate constants for adiabatic ET and PCET reactions using a generalized GCE Marcus-like [75] empirical valence bond theory (GCE-EVB). The non-adiabatic ET and PCET rate constants are derived using a golden-rule formalism within GCE. The theoretical work results in ET and PCET rate constants valid for both adiabatic and non-adiabatic (proton-coupled) electron transfer rates and the inclusion of proton tunneling in PCET. The developed rate theories can readily be combined with modern computational methods based on (GCE-)DFT. The derived rate equations form the basis for treating electrocatalytic kinetics and combining them with (GCE-)DFT methods expands the type of systems, conditions, and phenomena in electrocatalysis amenable for first principles modelling.

The paper is organized as follows. In Section 2 a general rate theory and TST within GCE are developed. Rest of the paper focuses on ET and PCET kinetics using GCE-TST. Section 3 shows how the adiabatic barrier and rate of ET and PCET reactions are computed using GCE-EVB and free energy perturbation theory within GCE leading to a fixed potential version of Marcus theory. Tafel slopes and other use quantities as extracted from GCE-EVB are analyzed. Finally, in section 4 non-adiabatic rate constants for ET and PCET reactions with generalized first-principles Hamiltonians and many-electron wave functions.

2. Rate theory in the grand canonical ensemble

As highlighted in the preceding discussion, the electrode potential is expected to affect the energetics and kinetics in complex ways. Thus, the potential should be treated explicitly rather than as a simple corrective parameter as often done in theoretical and computational models used in electrocatalysis. Formulating all expectation values within GCE naturally includes the electrode potential from the start and this forms the basis for the methods developed here and building on our previous grand canonical multi-component DFT[3]. The key is that the electrode potential is included in the *ab initio* Hamiltonian within the GCE and as results all observables and quantities depend explicitly on the potential. For details on GCE, see Appendix B and previous work in Ref.3.

To extend (micro)canonical rate theory to the GCE, only particle conserving reactions are considered. Thus, only a state with N particles can be converted to state with N particles but the population and probability of N particle states is determined by the GCE density operator. Hence, all equilibrium quantities are always well-defined but jumps between states with unequal number of particles are suppressed. In general this is not expected to limit the applicability of the rate expressions derived in this work; if a quantum system is characterized by particle conserving operators ($\hat{H}$ Hamiltonian, $\hat{S}$ entropy, and$\hat{N}$ particle number), even time-dependent observables are obtained as ensemble weighted expectation values from $O(t) = \mathrm{Tr}\left[\hat{\rho}\hat{U}(t_0,t)\hat{O}(t)\hat{U}(t,t_0)\right] = \sum_n p_n \langle\psi_n|\hat{U}(t_0,t)\hat{O}(t)\hat{U}(t,t_0)|\psi_n\rangle$ which do not include changes between states with different number of particles.[76] Hence, even explicit propagation of the wave function does not allow sudden jumps in particle numbers or jumps between states between different number of particles.

In a similar way, particle fluxes needed for the flux formulation of rate theory (see below) can be applied within the GCE as long as (local) equilibrium is maintained. This implies that the Hamiltonian is time-independent and that only particle conserving reactions contribute to the rate constant according to the grand canonical distribution[77]. Furthermore, computation of correlation functions and hence fluxes poses both theoretical and computational difficulties. While both may in principle be directly computed within GCE[77], the computation includes the coupling of the system to the particle reservoir and introduces the reservoir time scales. Also, the sampling needs to account for trajectories for which the particle number is equal at

times t and $t+\tau$. This is because in GCE the phase space volume is not globally conserved and Liouville theorem does not hold. As a result, the computed ensemble properties will depend on time if the system is not in equilibrium i.e. the phase distribution function $\rho(\mathbf{q},\mathbf{p},N,t)$ is not stationary i.e. if $d_t\rho(\mathbf{q},\mathbf{p},N,t) \neq 0$[77–79] ($\mathbf{p}$ and $\mathbf{q}$ are momentum and position, respectively). In the context of the present work it is important to notice that both equilibrium ($d_t\rho(\mathbf{q},\mathbf{p},N,t) = 0$ at $t \to \infty$) and instantaneous ($\lim_{t\to 0^+}$) properties are uniquely defined by the GCE[77, 79]; both qualities are absolutely essential in order to formulate the rate and transition state theories within GCE.

Herein only equilibrium and instantaneous quantities are used. Intermediate times would require running GCE-dynamics or making assumptions on the reservoir-system couplings. Hence, non-equilibrium processes cannot be treated using the approaches presented in this paper. Another limitation of the current approach is that kinetics of electron transfer from the electron "bath" degrees of freedom are not included and are therefore assumed sufficiently fast. Neither of these limitations are not expected greatly limit the applicability of the approach for electrocatalytic or electrochemical reactions. In these reactions the electron bath is provided by a conducting electrode and equilibrium conditions are controlled by constant temperature and potential which also provide the natural control parameters in the GCE utilized in this work. It is noted that mass transfer in electrochemical systems is not in equilibrium or even steady-state. However, the reaction rate coefficients are independent of particle fluxes and concentrations and therefore the elementary rate constants can be characterized by their equilibrium values as long as the Hamiltonian of the quantum part is time-independent and particle conserving.

After establishing the particle conserving and equilibrium nature of the rate constants, the GCE rate constants can be formulated. To allow various types of reactions to be described, the canonical rate expression due to Miller[61–63, 69] is used:

$$k(T,V,N)Q_I = \int dE P(E) \exp[-\beta E] \tag{1}$$

where $P(E)$ is the transition probability at a given energy, Q_I is the canonical partition function of the initial state, and $\beta = (k_B T)^{-1}$. This formulation can be expressed in several equivalent forms and below these different flavors are referred to as the flux correlation formulation.[62]. Im-

posing the particle conservation of wave functions and equilibrium lead to grand canonical reaction rate of the form[62, 72]

$$\begin{aligned} k(T,V,\mu)\Xi_I &= \sum_{N=0}^{\infty} \exp[\beta\mu N] Q_0(T,V,N) k(T,V,N) \\ &= \sum_{N} \exp[\beta\mu N] \int dE P(E) \exp[-\beta E] \\ &= \sum_{N=0}^{\infty} \exp[\beta\mu N] \lim_{t\to\infty} C_{fs}(t) \end{aligned} \tag{2}$$

where $\Xi_I = \exp[\beta\mu N] Q_I$ is the initial state grand partition function and where $C_{fs}(t)$ is either the quantum or classical flux-side correlation function in the canonical ensemble, see below. Above N is the number of species (nuclear or electronic) in the system. Based on the discussion above, only the $t \to 0^+$) and $t \to \infty$ should be considered for the flux-side correlation function in the rate expressions.

While the above equations are completely general and various flavors of rate theories can be extracted by invoking different Hamiltonians and transition probabilities, they are somewhat cumbersome to treat. Indeed, it would be convenient if the GCE could be used directly to evaluate the rate without explicitly sum over different particle numbers. Moving towards but still retaining maximum generality, it is assumed that the nuclei follow classical trajectories. While this might seem like a drastic assumption, Feynman[80] has shown that quantum mechanics can be formulated using classical trajectories as long all possible paths are included. Indeed, the use of Feynman's path integral methodology is behind several quantum mechanical rate theories[81]. Using a classical Hamiltonian and suppressing non-adiabatic effects by using a a single potential energy surface (PES), the flux-side correlation can be written in the ring-polymer form as[81]

$$C_{fs}(t) = \frac{1}{(2\pi\sim)^f} \int d\mathbf{p}^f d\mathbf{q}^f \exp(-\beta_n H_n) \delta[f(\mathbf{q})] \dot{\mathbf{q}} h[f(\mathbf{q}_t)] \tag{3}$$

where n is the number of beads, $\beta_n = \beta/n$, $f = Nn$, $H_n = \sum_{i=1}^{N} \sum_{j=1}^{n} \frac{|\mathbf{p}_{i,j}|^2}{2m_i} + \frac{1}{2}|\mathbf{q}_{i,j} - q_{i,j-1}|^2 + \sum_{i=1}^{n} V(q_{1,i}...N, i)$. Above, $\delta[f(\mathbf{q})]$ constrains the trajecto-

ries to start from the dividing surface, $\dot{\mathbf{q}}$ is the initial flux along the reaction coordinate, and $h[f(\mathbf{q}_t)]$ is the side function which includes the dynamic information whether a trajectory is reactive or not. Also, the non-adiabatic reactions can be described using a Hamiltonian with several coupled PESs and by using side function h which projects the state on different PESs. [82, 83]. At the classical limit $T \to \infty$ and $\beta_n \to 0$ leads to the shrinkage of the ring-polymer to a single bead. At this limit $C_{fs}(t)$ obtains its correct classic limit. In principle, $C_{fs}(t)$ within GCE can be directly computed with nuclear quantum and non-adiabatic effects using ring polymer molecular dynamics[84] but this is not within the scope of the present work.

Next transition state theory (TST) assumption is made[61–63]. In TST, the instantaneous $\lim_{t\to 0_+} C_{fs}(t)$ is considered corresponding to the assumption that there are no-recrossings of the dividing surface. Note that TST in this form is valid for non-adiabatic reactions as well if several PESs are used for computing C_{fs}. While a general, rigorous quantum TST has proven difficult to obtain due to the non-commuting nature of the flux and Hamiltonian operators, recent work has shown that the zero-time dynamics lead to ring-polymer TST which can be considered as a quantum TST.[65, 66] Furthermore, the path integral QTST[68] and its harmonic approximation (the popular semi-classical instanton rate theory in its ring polymer form[67, 85]) also arise from the path integral presentation of quantum mechanics. Both quantum/classical and adiabatic/non-adiabatic TSTs are written as

$$k_{TST}(T,V,N)Q_0(T,V,N) = \lim_{t\to 0_+} C_{fs}(t) \tag{4}$$

and the exact rate is recovered by introducing a correction

$$\begin{aligned} k(T,V,N) &= \lim_{t\to\infty} \kappa(t) k_{TST}(T,V,N) \\ \text{with} \quad \kappa(t) &= \frac{C_{fs}(t)}{C_{fs}(t\to 0_+)} \end{aligned} \tag{5}$$

where $\kappa(t)$ is the time-dependent transmission coefficient. For long-times, it can also be written as $\kappa = k(T,V,N)/k_{TST}(T,V,N)$.[86] Inserting this equation in Eq.(2) can be used to compute the most general grand canonical rate constant.

The above treatment is very general and needs further simplification to enable facile computation of reaction rates within the GCE. Here I will con-

centrate only on classical nuclei and then instead of working with the flux-side correlation function it is easier to write the rate in terms of the cumulative reaction probability of Eq. (2). For classical nuclei, the general rate equation in the GCE is written in terms of the time-integral of the flux correlation function was contains all the dynamic information[62, 63]: $P_r(\mathbf{p},\mathbf{q}) = \lim_{t\to\infty} h[f(\mathbf{q}_t)] = \int_0^\infty dt \frac{d}{dt} h[f(\mathbf{q}_t)] = \int_0^\infty dt C_{ff}(\mathbf{q}_t, \mathbf{p}_t)$.

$$
\begin{aligned}
k(T,V,\mu)\Xi_I &= \sum_{N=0}^{\infty} \exp[\beta\mu N] \int dE P_{cl}(E) \exp[-\beta E] \\
&= \sum_{N=0}^{\infty} \exp[\beta\mu N] \int \frac{d\mathbf{p}d\mathbf{q} \exp[-\beta H(\mathbf{p},\mathbf{q})] F(\mathbf{p},\mathbf{q}) P_r(\mathbf{p},\mathbf{q})}{(2\pi\sim)^N} \\
&= \sum_{N=0}^{\infty} \exp[\beta\mu N] \int \frac{d\mathbf{p}d\mathbf{q} \exp[-\beta H(\mathbf{p},\mathbf{q})] F(\mathbf{p},\mathbf{q}) \int_0^\infty dt C_{ff}(t)}{(2\pi\sim)^N} \\
&\approx \sum_{N=0}^{\infty} \exp[\beta\mu N] \frac{k_B T}{h} Q^\ddagger \int dt \delta(t) = \sum_N \exp[\beta\mu N] \frac{k_B T}{h} Q^\dagger \\
&\equiv \frac{k_B T}{h} \Xi^\dagger
\end{aligned}
\tag{6}
$$

where on the second last line making the short time approximation[63] to $C_{ff}(t \to 0) = \frac{k_B T}{h} Q^\ddagger \delta(t)$ leads to the TST expression. Above, $P_{cl}(E)$ denotes transition probability for classical nuclei but the electrons are of course quantum mechanical[59, 72]. The result on the last line of the previous equation, shows that the structure of GCE-TST and canonical TST have similar structures. A similar conclusion was also derived by Chandler in Ref.87 if memory effects are neglected. To obtain the GCE rate constant without invoking the TST approximation one can use the transmission coefficient to write

$$
k(T,V,\mu)\Xi_I = \sum_{N=0}^{\infty} \exp[\beta\mu N] \kappa(T,V,N) \frac{k_B T}{h} Q^\ddagger \approx \langle \kappa_\mu \rangle \frac{k_B T}{h} \Xi^\ddagger \tag{7}
$$

where it is assumed that the transmission coefficient is insensitive to changes in the particle number and $\langle \kappa_\mu \rangle$ is the effective transition probability. To complete the derivation for the classical GCE rate constant, the rate is expressed in terms of grand energies

$$
\begin{aligned}
k(T,V,\mu) &= \langle\kappa_\mu\rangle \frac{k_B T}{h} \exp\bigl[-\beta(\Omega^\ddagger - \Omega_I)\bigr] \\
&= \langle\kappa_\mu\rangle \frac{k_B T}{h} \exp\bigl[-\beta\Delta\Omega^\ddagger\bigr]
\end{aligned}
\tag{8}
$$

where the definition $\Omega_i = -\ln(\Xi_i)/\beta$ has been used. Above the only new assumption besides grand canonical equilibrium distribution and the TST, is that the flux out of the transition state does not depend on the number of particles in the system. For large enough systems and small variations in the particle this a well justified assumption. What is achieved is a fixed chemical potential rate equation where the rate is determined by the grand free energy barrier. The transmission coefficient needs to be approximated but this depends on the case at hand. The harmonic GCE-TST expression for the fully open system is derived in Appendix C resulting in Eq (C.4).

2.1. Allowing only the electron number to fluctuate

The general development above is valid when both nuclear and electronic subsystems are open. A significant simplification results if the number of nuclei is not allowed to fluctuate and the system is open only for electrons. This is also the typical scheme used in first principles modelling within GCE. Harmonic TST rates for constant number of nuclei and constant electrochemical potentials are derived in Appendix C.

Fixing only the electron chemical potential gives a semi-grand canonical ensemble used for deriving the thermodynamics of electrocatalytic system in Ref. 3. Using the same semi-GCE to kinetics, is used herein to derive rate equations as a function of electrode potential. *From now on, only the numbers of electrons is allowed to fluctuate and the state of the system is determined by T, V, number of nuclei N_N, chemical potential of the electrons μ_n, and number of electrons in the system N unless explicitly specified otherwise.*

3. Adiabatic barriers and rates from GC-EVB

To compute the GCE-TST rate at some electrode potential, the grand energy barrier of Eq. (8) needs to be obtained. For adiabatic reactions methods like the constant-potential[20] nudged elastic band[88] can be used. However, usually one is interested in rates as a function of the electrode potential and, hence, the barriers needs to be obtained for a range of electrode

potentials which is computationally expensive. Another possibility is for computation of the grand energy barrier, is to extend the adiabatic Marcus theory[75] to the GCE. Marcus theory can be viewed as special case of the empirical valence bond (EVB) theory[89] commonly utilized in electron[75] and proton transfer theories.[53, 89–92]. As shown below, the GCE-EVB theory has the advantage, that the adiabatic barrier needs to be explicitly computed only for at a single electrode potential. Barriers at other potentials can be obtained using well-defined interpolation of Eq.(22).

In these EVB and Marcus theories the initial and final states are presented using diabatic states, effective wave functions and free energies[75]. This can be extended to GCE by using two effective, fixed potential surfaces which can be understood as a statistical mixture of states with probabilities given by the density operator in GCE (see Appendix B and our previous work in 3). Importantly, the diabatic ground states obtained using the GCE density operator naturally include many-body states of coupled electrode-reactant-solvent system and the complexity of the electrochemical interface is implicitly included in the model. Also, there is no need to decompose the rate constants to orbital dependent quantities; in the current GCE formulation, the redox-molecule and the electrode are fully coupled and the total wave function $|r, \mathbf{e}\rangle$ is treated as a single entity in (see Appendix A for additional discussion). Then, two grand canonical diabatic all-electron wave functions are used to form an effective diabatic GCE Hamiltonian. This is analogous to molecular Marcus theory in which the canonical diabatic Hamiltonian comprises of an initial (oxidized) I and final(reduced) molecule F.

To form the GCE diabatic states, the work of Reimers[93, 94] on canonical ensembles is followed. As noted by Reimers, the density matrix $\hat{\bar{\rho}}$ can be written using either adiabatic or non-adiabatic states. Especially, when only two electronic states are used, the connection of the Born-Huang expansion bears striking resemble to the commonly used 2×2 diabatic Hamiltonians used for deriving electron transfer rate theory. In the canonical ensemble, the diabatic states are ϕ_I and ϕ_F corresponding to the electron localized on the initial (I) or final (F) state while the molecular electronic-vibrational Hamiltonian is

$$H_{dia}(N, V, T) = \begin{bmatrix} H_{II} & H_{IF} \\ H_{FI} & H_{FF} \end{bmatrix} \tag{9}$$

with

$$H_{II}(R) = \langle\phi_I|\hat{H}_{el}(R)|\phi_I\rangle + \hat{T}_{nuc} = E_I + \hat{T}_{nuc} \tag{10a}$$

$$H^*_{FI} = H_{IF} = \langle\phi_I|\hat{H}_{tot}(R)|\phi_F\rangle \tag{10b}$$

$$H_{FF} = \langle\phi_F|\hat{H}_{el}(R)|\phi_F\rangle + \hat{T}_{nuc} = E_F + \hat{T}_{nuc} \tag{10c}$$

where $\hat{T}_{nuc}$ is the nuclear kinetic energy operator, $\hat{H} = \hat{H}_{el} + \hat{T}_{nuc}$, and H_{el} includes electron kinetic energy and Coulomb energies of the electron-nucleus system. The Born-Huang, or vibronic, states are

$$\begin{aligned}\Psi_i(R) &= \sum_j [C^I_{ij}\,|\psi_I\rangle\,|\chi_j\rangle + C^F_{ij}\,|\psi_F\rangle\,|\chi_j\rangle] \\ &= \sum_{k=I,F} |\psi_k\rangle \sum_j C^I_{ki,j}\,|\chi_j\rangle\end{aligned} \tag{11}$$

where Ψ, ψ, and χ are the vibronic, electronic, and nuclear wave functions, respectively. C is the weight of each state. Using these definitions the, density matrix for a canonical ensemble is

$$\rho(N,V,T) = \begin{bmatrix}\rho_{II} & \rho_{IF} \\ \rho_{FI} & \rho_{FF}\end{bmatrix} \tag{12}$$

with $\rho_{AB} = \sum_j C^A_{ji} C^B_{ji}$ and the total density matrix has dimension $(2 \times N_i) \times (2 \times N_i)$.

Next the diabatic canonical Hamiltonian is generalized to the grand canonical ensemble. To simplify the notation, it is assumed that the initial and final can approximated as a single electronic state and a single vibrational state - extension to include more vibrational state is straight-forward. Then, the total vibronic state is written as $\Psi(\mathbf{R}) \approx c_I\,|\psi_I\rangle\,|\chi_I\rangle + c_F\,|\psi_F\rangle\,|\chi_F\rangle$. In electron transfer theory the vibronic states are often assumed to be harmonic but here such an assumption is not needed. Next, the total number of electrons is allowed to fluctuate while the electron Fermi-level is fixed. These are effectively introduced by using the equilibrium reduced density operator within the GCE [3] (see also Appendix B)

$$\begin{aligned}&\hat{\bar{\rho}}_{red} = \sum_N p_N \sum_{ij} |\Psi_{Ni}\rangle\,\langle\Psi_{Nj}| \\ &\text{with} \quad |\Psi_i\rangle = c_I\,|\psi_I\rangle\,|\chi_I\rangle + c_F\,|\psi_F\rangle\,|\chi_F\rangle\end{aligned} \tag{13}$$

where p_N is the GCE weight for a state with N electrons. The resulting density matrix will have N-dimensional block-diagonal form with 2×2 blocks. Similarly the Hamiltonian matrix is made of Eq.(9) H^N_{dia} blocks. Diagonalizing each block separately will give canonical adiabatic states whereas $\mathrm{Tr}\left[\hat{\bar{\rho}}_{red}\hat{H}\right]$ gives the adiabatic grand canonical free energy. Because the trace is cyclic, both $\hat{\bar{\rho}}_{red}$ and $\hat{H}$ can be reorganized which keeps the (diabatic) free energy unchanged as long as diagonal elements remain at the diagonal. This freedom is utilized to reorganize the matrix so that the upper part of $\hat{\bar{\rho}}_{red}$ and $\hat{H}$ correspond to the initial state and the lower part to the final diabatic states. Tracing the upper and lower parts separately, diabatic GC free energies of initial and final states (Ω_{II} and Ω_{FF}) are obtained. The adiabatic energy is computed by diagonalizing a 2×2 GCE Hamiltonian.

$$H_{GCE-dia} = \begin{bmatrix} \Omega_{II} & \Omega_{IF} \\ \Omega_{FI} & \Omega_{FF} \end{bmatrix} \tag{14}$$

where the diagonal elements are the grand energies of the oxidized (II) and reduced (FF) systems. The off-diagonal elements account for the interaction and mixing of the initial and final states. As written here, they can be understood in the framework of empirical valence bond (EVB) theory[89] commonly utilized in electron[75] and proton transfer theories.[53, 89–92] In this, way the off-diagonal elements can be fitted so that diagonalization of Eq.(14) produces the adiabatic grand canonical potential energy surface. Hence, the above methodology might be called GCE-EVB approach.

Finally, note that the (diabatic) grand canonical states correspond to a single electron density which are guaranteed theory to be unique for a given electrode potential by the Hohenberg-Kohn-Mermin[3, 4]. The only disambiguity is the definition of these diabatic states. In principle it is also possible to add other, possibly excited states as basis states. In practice the GCE diabatic energies,(Ω_{II} and Ω_{FF}), can be computed directly by applying using *e.g.* constrained DFT[95–97] with fixed potential DFT. Below it is shown how the grand canonical free energies can be obtained from atomistic simulations.

3.1. Computation of diabatic GCE surfaces and barriers

An approach often used in molecular simulations for constructing the diabatic free energy curves is to sample the diabatic potentials along a suitable reaction coordinate. For ET, PT, and PCET reactions in the canon-

ical ensemble this coordinate is the energy gap between the two diabatic states as shown by Zusman[98] and Warshel[99]: $\Delta E_{gap}(R) = E_F(R) - E_I(R)$.[78, 100] From the sampled energy gap the free energy curves are obtained as $A(R) = -k_B T \ln(p(E_{gap}(R))) + c$. If the distribution is Gaussian ($p(E_{gap}(R)) = c\exp[-(\Delta E_{gap} - \langle \Delta E_{gap} \rangle)^2/2\sigma^2]$) and the resulting free energy curves a parabolic. The barrier in EVB or Marcus theory is then obtained from the intersection of the initial and final diabatic curves[100–103]. Within GCE, the energy cap is simply $E_{gap}(R;\mu) = \sum_{N,i} p_{N,i} E_{gap}(R_i, N)$. The gap distributions can be formulated and computed by generalizing Zwanzig's[104] the canonical free energy perturbation theory to the GCE. This route provides a rigorous way to derive the reaction barrier in terms of diabatic states and energies as presented in Appendix D.

The reaction energy barrier can be computed from the initial-final state energy gap distribution functions using[99, 105–110]

$$k_{IF} = \kappa \frac{\exp\left[-\beta g_I(\Delta E^\ddagger)\right]}{\int d\Delta E \exp[-\beta g_I(\Delta E)]} = \kappa p_I(\Delta E^\ddagger) \tag{15}$$

where $g_i(\Delta E)$ is the free energy curve in state i as a function of the energy gap, $p_I(\Delta E^\ddagger)$ is the gap distribution at the transitions state, and κ denotes an effective pre-factor. The above shows that the reaction rate is determined by the energy gap distribution function $p^I(\Delta E) = \langle \delta(\Delta E(R) - \Delta E) \rangle_I$ from Eq. (D.6).

When assuming that $E_{gap}(R;\mu)$ is Gaussian, the GC-diabatic states are parabolic and the Marcus barrier in GCE is given by Eq. (18). As shown in the Appendix C and Section 4 for the GCE-NATST, the (Gaussian) gap distribution may be derived using a (second order) cumulant expansion. This results in gap distribution of the following form

$$p_I(\Delta E) = \frac{1}{\sqrt{2\pi\sigma_I}} \exp\left[-\frac{(\Delta E - \langle \Delta E \rangle_I)^2}{2\sigma_I^2}\right] \tag{16}$$

where $\langle \Delta E \rangle_I$ is the energy gap expectation value in the initial state obtained from Eq. (D.6) and $\sigma_I = \langle (\Delta E)^2 \rangle_I - (\langle \Delta E \rangle_I)^2$ is the gap variance. The Marcus relation is then obtain after standard manipulations[100, 106] by inserting these relations in Eq. (D.8) to give

$$p_I(\Delta E^\ddagger) = \frac{1}{\sqrt{4k_B T \Lambda}} \exp\left[-\beta \frac{(\Delta\Omega_{FI} + \Lambda)^2}{4\Lambda}\right] \tag{17}$$

where $\sigma_I^2 = \sigma_F^2 = 2k_BT\Lambda = k_BT(\langle \Delta E \rangle_I - \langle \Delta E \rangle_F)$, Λ is the reorganization grand energy and and $\Delta\Omega_{FI} = \frac{1}{2}(\langle \Delta E \rangle_I + \langle \Delta E \rangle_F)$ is the reaction grand energy as depicted in Figure3.1. Finally, the Marcus expression within GCE is

$$k = \frac{\kappa}{\sqrt{4k_BT\Lambda}} \exp\left[-\beta \frac{(\Delta\Omega_{FI} + \Lambda)^2}{4\Lambda}\right] \tag{18}$$

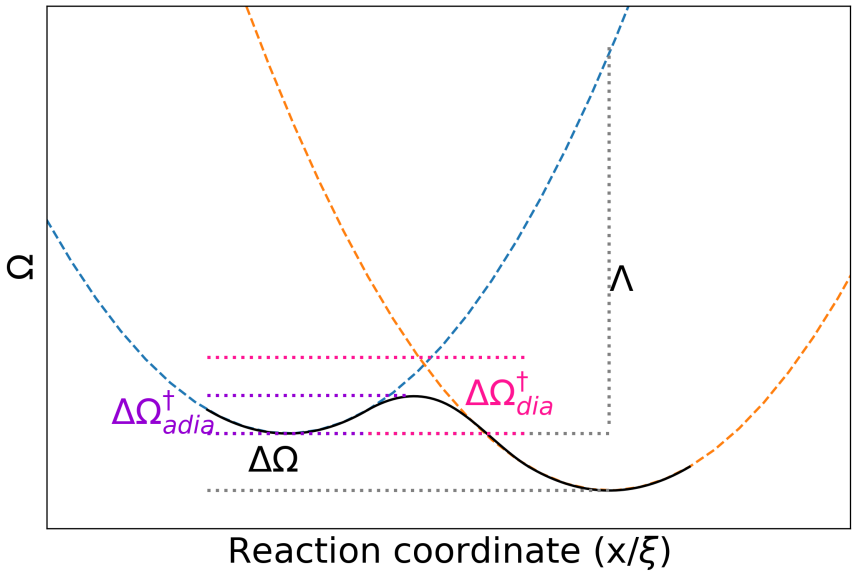

Figure 2: Schematic depiction of the important GCE-EVB quantities. The blue (orange) dashed lines is initial (final) diabatic surface while the black solid line is the adiabatic surface.

The energy barrier of Eq. (18) is the diabatic energy barrier. The adiabatic barrier can the be computed using Eq. (14) as discussed in Section. 3.2 below. One caveat the keep in mind is more involved within the GCE than the canonical ensemble as shown in Section 4. The above result may safely be used when $\kappa \approx 1$ for all particle numbers meaning that the reaction is always fully adiabatic.

3.2. Implications of the canonical GCE-EVB rate theory

For symmetric grand energy surfaces the diabatic grand energy barrier can be is estimated from the crossing point of the two quadratic grand energy surfaces with equal curvatures is given in Eq. (18). The requirement of equal curvature can be relaxed following Mattiat and Richardson[74], who compute the reorganization energies for both the initial and final states Λ_I and Λ_F, respectively. Then the asymmetry parameter may be defined as

$$\alpha_{as} = \frac{\Lambda_I - \Lambda_F}{\Lambda_I + \Lambda_F} \tag{19}$$

and the transition state is located at the crossing point

$$x^{\ddagger}/\xi = -\frac{1}{\alpha_{as}} + \frac{1}{\alpha_{as}}\sqrt{1 - \alpha_{as}\left(\alpha_{as} + \frac{4\Delta\Omega}{\Lambda_I + \Lambda_F}\right)} \tag{20}$$

Using these definitions the asymmetric diabatic Marcus barrier and rate are obtained as

$$\Delta\Omega^{\ddagger} = \frac{1}{4}\Lambda_I \left(x^{\ddagger}/\xi - 1\right)^2 \tag{21a}$$

$$k \approx \frac{\kappa}{\sqrt{4k_B T \Lambda_I}} \frac{1 + \alpha_{as}}{1 + \alpha_{as} x^{\ddagger}/\xi} \exp\left[-\beta\Delta\Omega^{\ddagger}\right] \tag{21b}$$

If $\alpha_{as} \to 0$, the regular Marcus rate and barrier are obtained. In Fig.3.2 the effect of asymmetry and reaction energy to the reaction barrier and location of the transition state are compared. It can be seen that both the barrier heights and its location are affected by the asymmetry and reaction energy.

The above equations enable a theoretically justified way to compute or predict the reaction barrier at a given electron chemical potential using just few parameters: Λ and $\Delta\Omega$. Both the barrier height and shifts in its location can be determined. Furthermore, it is not necessary to find the transition state geometry as long as all the parameters can be computed. The practical computations can be made using *e.g.* fixed potential implementations diabatic electronic structure methods such as the constrained DFT[95–97] The grand energy curves in Figure 3.2 qualitatively reproduce the DFT computed reaction free energy barriers for HER[20] and CO_2 reduction[38].

The adiabatic reaction barrier can be extracted from the non-adiabatic barrier obtained by diagonalizing Eq.(14) or from .(18) by introducing an

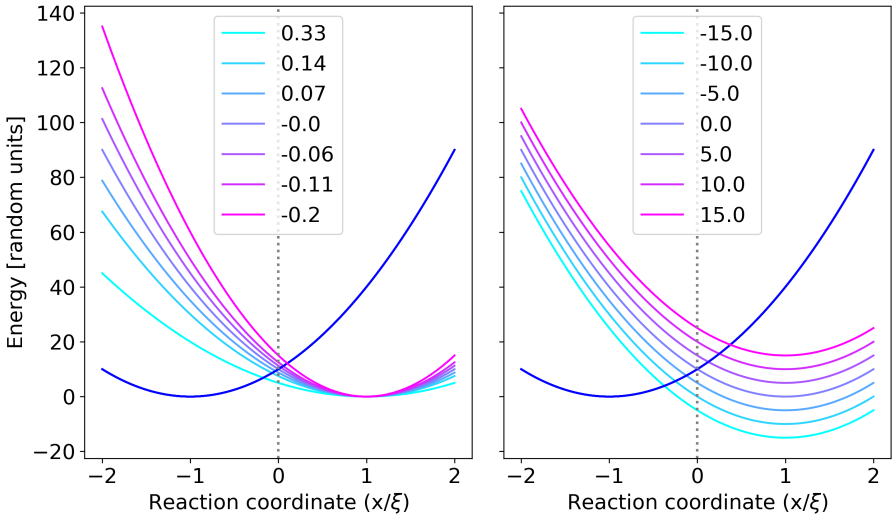

Figure 3: **Left**: EVB curves at different different asymmetries α_{as}. The initial state reorganization energy is $\Lambda_I = 40$ while the final state reorganization energy $\Lambda_F \in [20, 60]$. The reaction energy is $\Delta\Omega = 0$ for all curves. **Right**: EVB curves as a function of the reaction energy: $\Delta\Omega \in [-15, 15]$. For all curves $\Lambda_I = \Lambda_F$. **Both**: The dashed line at $x = 0$ indicates the position of the transition state when $\Lambda_I = \Lambda_F$ and $\Delta\Omega = 0$. The curve crossing point equals $\Delta\Omega^{\ddagger}_{dia}$

adiabaticity correction. For the canonical ensemble, this correction is known as the Hwang-Åqvist-Warshel equation[111]. If the GCE-diabatic states are quadratic along the reaction coordinate and share the same curvature along the reaction coordinate, the adiabatic barrier can be written as [111, 112]

$$\begin{aligned} \Delta\Omega^{\ddagger}_{ad,EVB} &= \frac{(\Delta\Omega + \Lambda)^2}{4\Lambda} - \Omega_{IF}(x^{\ddagger}) + \frac{(\Omega_{IF}(x^I))^2}{\Delta\Omega + \Lambda} \\ &= \Delta\Omega^{\ddagger}_{dia} - \Omega_{IF}(x^{\ddagger}) + \frac{(\Omega_{IF}(x^I))^2}{\Delta\Omega + \Lambda} \end{aligned} \tag{22}$$

where Ω_{IF} is the off-diagonal matrix of the GCE-EVB Hamiltonian in Eq. (14). If the Condon approximation is used, the above equation is greatly simplified as $\Omega_{IF} \approx \Omega_{IF}(x^{\ddagger}) \approx \Omega_{IF}(x^I)$. From a practical perspective it is interesting to observe how the adiabatic GCE-EVB barrier changes when the parameters a changed. From the schematics shown in Figures 3.1 and 3.2, one can observe that changes of the minima along the reaction coordinate

correspond to horizontal displacements of the diabatic states and and changes in Λ. Vertical changes correspond to changes in the reaction grand energy $\Delta\Omega$. Usually one concentrates only on changes in the free energy as reorganization coordinate not expected change for similar reactions or different electrode potentials (this assumptions is also made in Section 4.) Focusing on the reaction grand energy, it is easy show that under equilibrium conditions, $\Delta\Omega = 0$, the barrier is given by

$$\Delta\Omega^{0,\ddagger}_{ad,EVB} = \frac{\Lambda}{4} - \Omega_{IF} + \frac{(\Omega_{IF})^2}{\Lambda} \approx \frac{\Lambda}{4} - \Omega_{IF} \tag{23}$$

which leads to $\Lambda = 4(\Delta\Omega^{0,\ddagger}_{ad,EVB} + \Omega_{IF}) \approx 4\Delta\Omega^{0,\ddagger}_{dia}$ assuming that $\Omega_{IF} << \Lambda$. The equilibrium point is characterized by zero over-potential $\eta = \Delta\Omega = 0$. Replacing the solution for Λ in Eq. (22) gives the diabatic barrier as

$$\Delta\Omega^{\ddagger}_{dia} = \Omega^{0,\ddagger}_{dia}\left(1 + \frac{\Delta\Omega}{4\Omega^{0,\ddagger}_{dia}}\right)^2 = \Delta\Omega^{0,\ddagger}_{dia} + \frac{\Delta\Omega}{2} + \frac{(\Delta\Omega)^2}{16\Delta\Omega^{0,\ddagger}_{dia}} \tag{24}$$

Inserting (24) in (22) results in the adiabatic reaction barrier as

$$\Delta\Omega^{\ddagger}_{ad,EVB} = \Delta\Omega^{0,\ddagger}_{ad,EVB} + \frac{\Delta\Omega}{2} + \frac{(\Delta\Omega)^2}{16\Delta\Omega^{0,\ddagger}_{dia}} \tag{25}$$

This result has several interesting implications and connections to previous work. The most immediate is that at small changes in the driving force $\Delta\Omega$, a linear dependence between the barrier and reaction energy is established. However, at larger driving forces, a non-linear dependence appears.

This can be directly translated to the language of electrochemistry by considering the changes in driving force as a function of the electrode potential or over-potential. As discussed by Trasatti[113, 114] and in our recent work[3], the absolute electrochemical potential and chemical potential are related by $E^M(abs) = E^M(red) + K$ with $E^M(red) = \Delta\phi^M_S - \mu^M_n$ where $E^M(red)$ is the reduced absolute potential, K is used to convert between different reference choices, $\Delta\phi^M_S$ is the Galvani potential difference between the metal M and solution S, and μ^M_n is the chemical potential of the electrode. Independent of the reference scheme, the changes in the electrode potential are directly related to the changes in the electrochemical potential of the electrons: $E^M(abs) \sim -\tilde{\mu}_n$. It is important to notice that for microscopic systems usually considered within GCE-DFT keeping $\tilde{\mu}_n$ fixed leads

to changes in the number of electrons in the initial and final states. As a result the canonical free energies $A(N)$ do not remain constant when change when $\tilde{\mu}_n$ is changed. Therefore, changes in the grand energy is in general $\delta\Omega = A(N_F;\tilde{\mu}) - A(N_I;\tilde{\mu}) - \tilde{\mu}_n(N_I - N_F)$.

$\delta\Omega$ may be extracted from constant potential calculations enabling the study of electrochemical kinetics as a function of the electrode potential: $-\partial r(T,V,\tilde{\mu}_n)/\partial\tilde{\mu}_n$ as done in a Tafel analysis, for example. The traditional measure in electrochemistry for reaction kinetics is the Tafel slope measuring how current is affected by changes in the over-potential. In heterogeneous and homogeneous catalysis the corresponding quantity is the Brønsted-Evans-Polanyi (BEP) coefficient or more generally (linear free) energy relations measuring the change of reaction rate when the reaction energy is changed. However, the work of Fletcher[115, 116] and Parsons[117] show that Tafel and BEP type analyses actually measure the same quantities; both measure the reaction rate as a function of the changes in the reaction driving force. For macroscopic electrochemical reactions the driving force is measured in terms of the over-potential while in microscopic calculations the driving force is the free energy. These two quantities are linked by $|\Delta\eta| = |\Delta\tilde{\mu}_n| = |\Delta\partial\Omega/\partial n|$.

Both the BEP and Tafel coefficients maybe computed from a single expression. The Tafel coefficient is defined as[2, 115, 116]

$$\alpha \propto \frac{\partial \ln k}{\partial E} = -\frac{\partial \ln k}{\partial \Delta\Omega}\frac{\partial \Delta\Omega}{\partial \tilde{\mu}_n}\frac{\partial \tilde{\mu}_n}{\partial E} = -\gamma\Delta\Omega' \tag{26}$$

where γ is BEP relationship and $\Delta\Omega'$ denotes the grand energy change as a function of the over-potential. Also $E \sim \tilde{\mu}_n$ has been used.

Let us focus first on the $\Delta\Omega'$ term which depends on the reaction and needs to be approximated. To facilitate this analysis, one recognizes that $\Delta\Omega = (A_F(\langle N_F\rangle) - A_I(\langle N_I\rangle) - \tilde{\mu}_n(\langle N_F\rangle - \langle N_I\rangle)$. For macroscopic systems, i) chemical reactions have $N_F = N_I$ while ii) simple electrochemical steps have $N_F = N_I \pm 1$. Then for chemical reactions $\Delta\Omega = \Delta A$ and the variation $\Delta\Omega'$ is expected to be small. For electrochemical reactions at the macroscopic limit, a particularly straightforward estimate is obtained from the computational hydrogen electrode (CHE) concept.[118] In the CHE model, the reaction energy $\Delta\Omega \approx \Delta A^0 \mp \eta$ for PCET steps with ΔA^0 computed without any bias potential. Hence, within CHE, $\alpha = \gamma$ for PCET steps and zero otherwise. Similar reasoning holds also for simple (outer-sphere) ET reactions in macroscopic systems as shown in Appendix E. For these reactions $\Delta\Omega \approx \Delta A^0 \mp$ constant $\times\, \eta$ and $\Delta\Omega' = \mp$constant.

For microscopic systems, however, such a simple relationship does not hold in general and models such as GCE-DFT can be used for computing $\Delta\Omega'$ explicitly. Thus far, $\Delta\Omega'$ has been reported in only few studies[20, 119]. In both works, $\Delta\Omega$ exhibits a roughly linear dependence on the applied potential. To conclude, $\Delta\Omega'$ is expected to be a constant close to unity for electrochemical reactions and close to zero for chemical reactions.

Next, the BEP γ of Eq (26) is analyzed. Using the diabatic barriers, one obtains

$$\begin{aligned}\gamma &= \left.\frac{\partial \ln k(T,V,\tilde{\mu}_n)}{\partial \Delta\Omega}\right|_{T,V} \\ &= \frac{\partial \ln \exp\left[-\beta\Omega^{\ddagger}\right]}{\partial\Delta\Omega} = \left[\frac{1}{2} + \frac{\Delta\Omega}{8\Delta\Omega^{0,\ddagger}_{dia}}\right] = \frac{1}{2}\left[1 + \frac{\Delta\Omega}{\Lambda}\right]\end{aligned} \tag{27}$$

From the above equation, it is seen that γ is not a simple constant but depends linearly on the reaction driving force. If the reorganization energy is small the dependence on the reaction grand energy becomes more pronounced. Based on the generalized BEP-Tafel energy identities the following relationships can be observed:

- If the quadratic part in Eq.(24) is neglected, one obtains the Butler-Volmer (BV) barrier. In this case the barrier depends linearly on the applied potential as $\Delta\Delta\Omega^{\ddagger}_{dia,EVB} \approx 0.5(A_F(\langle N_F\rangle) - A_I(\langle N_I\rangle) - \mu_{el}(\langle N_F\rangle - \langle N_I\rangle)$. μ_{el} is implicitly referenced against $\mu^{eq}_{el} = 0$ and can easily be converted to the over-potential $\mu_{el} - \mu^{eq}_{el} = \Delta\eta$. Note that $\Delta\Delta\Omega^{\ddagger}_{dia,EVB}$ is not expected to be linear for finite-sized systems.

  Again, for macroscopic systems $\langle N_F\rangle = \langle N_I\rangle$ and $\Delta\Delta\Omega^{\ddagger}_{dia,EVB} = \Delta\Delta A^{\ddagger}_{dia,EVB} = 0.5(A_F - A_I)$ which is the Brønsted-Evans-Polanyi result. The BV relationship is obtained by treating a specific reaction type. For example, in a typical ET, PT, or PCET the potential-dependent reaction free energy is given by $\Delta A = \Delta A(\eta = 0) \pm (n\eta)$. Using this for $\Delta\Delta A = \pm 0.5 n\eta$.

- Non-linearity of the grand energy barrier was already established above. For macroscopic systems non-linearity is established by including the quadratic part of the diabatic barrier in model. Lately[20, 36, 38] this has been observed computationally and it is pleasing that the GCE-EVB picture seems qualitatively correct.

A spectacular feature of canonical Marcus and EVB theory is the observation of an inverted region *i.e.* the rate constant starts to decline as the reaction becomes more exothermic. However, the inverted region has not been observed for electrochemical reactions even at large over-potentials. The grand canonical Marcus rate of Eq. (18) seems to predict an inverted region for highly exothermic conditions. However, as written in the Tafel equation (26) the rate as a function of the over-potential depends on both the change in A) barrier as a function of the reaction energy and B) change reaction energy as a function of the over-potential. A) would indeed predict an inverted region but B) suppress this if $\Delta\Omega \approx 0$. Then the Tafel slope would approach zero as predicted by the Marcus-Hush-Chidsey[120], Dogonadze-Levich-Kuztnetsov[49, 50], Newns-Anderson-Schmickler, Soudackov-Hammes-Schiffer[45] models of ET and PCET [51] (see also Appendix A). At the moment, there is not enough computational nor theoretical evidence on the behaviour of $\Delta\Omega$ as a function of the over-potential to predict or to analyze the Tafel slope any further.

To summarize, the generalized BEP-Tafel relationships has been derived from a microscopic perspective starting from a grand canonical rate theory. Both variation in the reaction energy barrier and the transition state location as a function of the potential can be predicted using just a few parameters. The general form of the BEP-Tafel relation is given in Eq. (26). For small over-potentials, the rate is expected to depend linearly on the applied potential. For larger over-potentials non-linear dependence is predicted, especially reactions for which the reorganization energy is small.

4. Non-adiabatic ET and PCET reaction rates within GCE

4.1. Non-adiabatic ET rate

As shown above, computation of adiabatic reaction rates from either GCE-HTST, GCE-EVB or GCE-perturbation theory do not yield any fundamental difficulties as compared to the canonical case; after finding the barrier, one can simply use a simple TST-like expression to compute the reaction rate using grand free energies. However, for a non-adiabatic process, using the grand free energy is not as straightforward. The main difficulty becomes from computation of the electronic transition matrix element which is not defined for states with different number of electrons. Hence, one cannot directly use the effective GCE-EVB states developed in Section 3 and

use them to compute the non-adiabatic rate. Instead, the electronic transition matrix element needs to be computed separately for each canonical transition. Afterwards, a summation over the canonical rates is performed to express the non-adiabatic ET/PCET rate as a expectation value. To obtain the non-adiabatic TST rate, the Golden-rule approach is used herein. In the canonical ensemble, the Golden-rule formulation of the rate is equivalent to Dogonadze's treatment.[49, 50, 101] Below theory for the computation of non-adiabatic ET and PCET rates within GCE is developed.

To start with, the electronic states $|iN\rangle$ are specified and they are eigenstates to the electronic Hamiltonian $\hat{H}_N^{el}$. Electronic states are defined for initial (i) and final (f) states with a fixed number of particles (N). Then the electronic energies for the initial and final states at fixed particle number at nuclear geometry Q are

$$\langle iN|\hat{H}_N^{el}|iN\rangle = \varepsilon_{iN}(Q) \quad \text{and} \quad \langle fN|\hat{H}_N^{el}|fN\rangle = \varepsilon_{fN}(Q) \tag{28}$$

Within the Born-Oppenheimer approximation (BOA), the nuclear wave functions and their energies ϵ in the initial ($|mN\rangle$) and final ($|nN\rangle$) electronic states are obtained from

$$\begin{aligned} [\hat{T}_Q + \varepsilon_{iN}(Q)]\,|mN\rangle &= \epsilon_{mN}\,|mN\rangle \quad \text{and} \\ [\hat{T}_Q + \varepsilon_{fN}(Q)]\,|nN\rangle &= \epsilon_{nN}\,|nN\rangle \end{aligned} \tag{29}$$

where $\hat{T}_Q$ is the nuclear kinetic energy. Within BOA, the total vibronic wave function and the corresponding energy factorize as

$$|imN\rangle = |iN\rangle\,|mN\rangle \quad \text{and} \quad E_{imN} = \varepsilon_{iN} + \epsilon_{mN} \tag{30a}$$

$$|fnN\rangle = |fN\rangle\,|nN\rangle \quad \text{and} \quad E_{fnN} = \varepsilon_{fN} + \epsilon_{nN} \tag{30b}$$

As the different energy contributions are additive, the canonical partition functions can be factorized:

$$\begin{aligned} Q_i^N &= \exp[-\beta\varepsilon_{iN}] \sum_m \exp[-\beta\epsilon_{mN}] \quad \text{and} \\ Q_f^N &= \exp[-\beta\varepsilon_{fN}] \sum_n \exp[-\beta\epsilon_{nN}] \end{aligned} \tag{31}$$

At this point all relevant canonical quantities have been defined and the focus turns to the GCE formulation of the Golden-rule rate. The GCE partition function for the initial state is

$$\Xi_i = \sum_N \exp[\beta\mu N] Q_i^N \tag{32}$$

This equation is inserted in the general GCE rate expression. For the non-adiabatic limit, the Golden rule rate is used. As shown in Appendix C and Appendix A, use of the Golden rule expression is consistent with the general rate theory based on the flux approach if the non-adiabatic Hamiltonian and suitable flux operator are utilized. The GCE-NATST rate constant is then

$$\begin{aligned} k_{GCE-NATST} &= \frac{2\pi}{\sim \Xi_i} \sum_N e^{-\beta(\varepsilon_{iN}-\mu N)} \sum_{m,n} e^{-\beta\epsilon_{mN}} \left| \langle Nnf|\hat{V}_N|imN\rangle \right|^2 \delta(E_{imN} - E_{fnN}) \\ &= \frac{2\pi}{\sim} \sum_N \sum_{m,n} p_{imN} \left| \langle Nnf|\hat{V}_N|imN\rangle \right|^2 \delta(E_{imN} - E_{fnN}) \end{aligned} \tag{33}$$

where p_{imN} is the population of the vibronic state $|imN\rangle$. Next, a significant simplification is made; it is assumed that the vibrational part of the canonical function does not depend on the number of electrons in the systems. This assumption gives $Q_i^N = \exp[-\beta\varepsilon_{iN}] \sum_m \exp[-\beta\epsilon_{mN}] \approx \exp[-\beta\varepsilon_{iN}] \sum_m \exp[-\beta\epsilon_m] = \exp[-\beta\varepsilon_{iN}] Q_m$ and the GCE partition function becomes

$$\Xi_i \approx Q_m \sum_N \exp[-\beta(\varepsilon_{iN} - \mu N] = Q_m \Xi_i \tag{34}$$

Inserting this approximation in the GCE-NATST rate expression gives

$$\begin{aligned} k_{GCE-NATST} &\approx \frac{2\pi}{\sim \Xi_i} \sum_N e^{-\beta(\varepsilon_{iN}-\mu N)} \sum_{m,n} \frac{e^{-\beta\epsilon_{mN}}}{Q_m} \left| \langle Nnf|\hat{V}_N|imN\rangle \right|^2 \delta(E_{imN} - E_{fnN}) \\ &= \frac{2\pi}{\sim} \sum_N p_{iN} \sum_{m,n} p_{mN} \left| \langle Nnf|\hat{V}|imN\rangle \right|^2 \delta(E_{imN} - E_{fnN}) \end{aligned} \tag{35}$$

where $p_{iN,el} = \exp[-\beta(\varepsilon_{iN} - \mu N)]/\Xi_{i,el}$ and $p_{mN} = \exp[-\beta\epsilon_{mN}]/Q_m$.

This equation has the structure of the canonical Golden rule rate weighted by the probability of being in the initial electronic state iN. To simplify the notation, one can momentarily concentrate only on the canonical part of the above rate expression. Using the Fourier transform presentation of the delta function, gives

$$\begin{aligned}
&\sum_{m,n} p_{imN} \Big| \langle Nnf|\hat{V}_N|imN\rangle \Big|^2 \delta(E_{imN} - E_{fnN}) \\
&= \frac{1}{2\pi\sim} \sum_{m,n} p_{imN} \Big| \langle Nnf|\hat{V}_N|imN\rangle \Big|^2 \int dt e^{it(E_{imN}-E_{fnN})/\sim} \\
&= \frac{1}{2\pi\sim} \sum_{m,n} p_{imN} \langle fmN|\hat{V}_N|inN\rangle \langle inN|\hat{V}_N|fmN\rangle \int dt e^{it(E_{imN}-E_{fnN})/\sim} \\
&\approx \frac{1}{2\pi\sim} \sum_{m,n} p_{imN} \Big| \langle fN|\hat{V}_N|iN\rangle \Big|^2 \int dt \langle mN|nN\rangle \langle nN|mN\rangle e^{it(E_{imN}-E_{fnN})/\sim} \\
&= \frac{1}{2\pi\sim} \sum_{m,n} p_{imN} V_{N,if}^2 \int dt \Big| \langle nN|mN\rangle_q \Big|^2 e^{it(E_{imN}-E_{fnN})/\sim} \\
&= \frac{V_{N,if}^2}{2\pi\sim} \int dt \left\langle e^{it(E_{imN}/\sim} e^{-it(E_{fnN})/\sim} \right\rangle_q = \frac{V_{N,if}^2}{2\pi\sim} \int dt C(t)
\end{aligned} \tag{36}$$

where $C(t)$ is an energy autocorrelation function. The last two equations are amenable to two different ways of computing the rate constant. The last can be used with a cumulant expansion approach, while the second last has the form of a thermally averaged Franck-Condon treatment. The cumulant expansion is presented in the main text while the Franck-Condon treatment is presented in Appendix G for completeness.

In the present work, nuclear degrees of freedom are treated classically. Following either Geva[121] or Marcus[122], the autocorrelation function can be expressed using a cumulant expansion[123]. Using the second order cumulant expansion results in

$$\begin{aligned}
&\langle \exp[iE_{fnN}t/\sim] \exp[iE_{imN}t/\sim] \rangle_i \approx \\
&\exp\left[\frac{-it}{\sim} \langle \Delta E_{fi}^N \rangle - \frac{1}{\sim^2} \int_0^t d\tau_1 \int_0^{\tau_1} d\tau_2 C(\tau_1 - \tau_2) \right]
\end{aligned} \tag{37}$$

where $\left\langle \Delta E_{fi}^N \right\rangle$ is the average free energy gap between the final and initial electronic diabatic states. Also $C(\tau_1 - \tau_2) = \left\langle \delta\Delta E_{fi}^N(\tau)\delta\Delta E_{fi}(0) \right\rangle$ where $\delta\Delta E_{fi}^N = \Delta E_{fi}^N - \left\langle \Delta E_{fi}^N \right\rangle$. $C(\tau_1 - \tau_2)$ is directly linked to the vibrational spectral density of the system[55, 101, 122, 124]. To obtain a manageable expression for the rate, the short time approximation or slow fluctuation limit[125] to the correlation function is used: $C(\tau_1 - \tau_2) \approx C(0) = \left\langle \delta(\Delta E_{fi}^N)^2 \right\rangle$. Inserting this in Eq. (37) yields

$$\exp\left[-\frac{1}{\sim^2}\int_0^t d\tau_1 \int_0^{\tau_1} d\tau_2 C(\tau_1 - \tau_2)\right] \approx \exp\left[-\frac{t^2}{\sim^2}(\left\langle \delta(\Delta E_{fi}^N)^2 \right\rangle\right] \tag{38}$$

This is inserted in Eq. (36) to give

$$\begin{aligned}
&\sum_{m,n} p_{imN} \left| \langle Nnf|\hat{V}_N|imN\rangle \right|^2 \delta(E_{imN} - E_{fnN}) \\
&\approx \frac{V_{N,if}^2}{2\pi\sim} \int_{-\infty}^{\infty} dt \exp\left[\frac{it}{\sim}\left\langle \Delta E_{fi}^N \right\rangle - \frac{t^2}{\sim^2}(\left\langle \delta(\Delta E_{fi}^N))^2 \right\rangle\right] \\
&= \frac{V_{N,if}^2}{2\pi\sim}\sqrt{\frac{2\pi\sim^2}{\left\langle \delta(\Delta E_{fi}^N)^2 \right\rangle}} \exp\left[\frac{-\left\langle \Delta E_{fi}^N \right\rangle^2}{2\left\langle \delta(\Delta E_{fi}^N)^2 \right\rangle}\right] \\
&\approx \frac{V_{N,if}^2}{2\pi}\sqrt{\frac{\pi}{k_B T\lambda}} \exp\left[-\frac{(\Delta E_{fi}^N + \lambda)^2}{4k_B T\lambda}\right]
\end{aligned} \tag{39}$$

where on the last line it has been assumed that the free energy surfaces are quadratic along the energy gap coordinate. The reorganization and reaction energies are defined as $\lambda = E_{im}(Q_F) - E_{fn}(Q_F)$ and $E_{fi}^N = E_{fn}^N(Q_F) - E_{im}^N(Q_I)$ (see Fig. 3.1). A generalization to asymmetric GCE-diabatic energy curves can be made following Mattiat and Richardson[74]. Furthermore, it is assumed that the curvature of the quadratic surfaces is the same for all particle numbers N in which case the reorganization energy does not depend on N. This should be to a rather good approximation as the reorganization is related to the reorientation of the surrounding medium which is expected be rather insensitive to the number of electrons in the system. For example, in the spin-boson model, which in the canonical ensemble yields the Marcus rate, the reorganization energy is only related to the bath frequencies in thermal equilibrium.[101] If the spin-boson model is applied to the present

GCE case, the vibrational, bosonic Hamiltonian would be assumed to be independent of the number of electrons and yield directly the reorganization energy which is indepenedent of the number of particle for the GCE. The assumption that the reorganization energy is independent on the particle number can also be reinforced by doing a re-derivation of the rate using the thermalized Franck-Condon approach as shown in the Appendix G.

Finally, the final GCE-NATST result is obtained by combining Eq. (35) with either Eq. (37) or (G.2) to give

$$k_{GCE-NATST}^{Marcus} = \sum_N p_{iN} \frac{V_{N,if}^2}{\sim\sqrt{4\pi k_B T \lambda}} \exp\left[-\frac{(\Delta E_{fi}^N + \lambda)^2}{4k_B T \lambda}\right] \tag{40}$$

The reorganization energy can also be separated to inner and outer sphere components as discussed in Section Appendix H. If this separation is invoked, one can alleviate the assumption that the total reorganization is independent of the particle number and instead assume that only bulk solvent (outer sphere) reorganization is a constant while the inner-sphere reorganization energy depends on the particle number.

4.2. PCET kinetics within GCE

The PCET kinetics is based on the PCET rate theory of Soudackov and Hammes-Schiffer. Within the canonical ensemble the relevant rate expressions were derived in Refs. 45, 53–55 and here this treatment is extended to the GCE yielding PCET rate constants at fixed electrode potentials. The PCET rate constant derivation follows a similar procedure as the one used above for the ET rates. In the case of PCET, an additional geometric variable q to denote the position of the transferring proton is introduced. Within BOA, the total vibronic wave function is then

$$|iumN\rangle = |iN(q,Q)\rangle\,|uN(Q)\rangle\,|mN\rangle \tag{41}$$

where it is explicitly written that the electronic wave function $|iN\rangle$ depends explicitly on the proton q and system coordinate Q while the proton wave function $|uN(Q)\rangle$ depends on the system coordinate Q. The wave functions and corresponding energies are solved using equations similar to the ET case

$$\begin{aligned} &\langle iN|\hat{H}_N^{el}|iN\rangle = \varepsilon_{iN}(q,Q) \quad \text{and} \\ &\langle fN|\hat{H}_N^{el}|fN\rangle = \varepsilon_{fN}(q,Q) \end{aligned} \tag{42a}$$

$$\begin{aligned}[\hat{T}_q + \varepsilon_{iN}(q,Q)]\,|iuN\rangle &= \epsilon^i_{uN}\,|iuN\rangle \quad \text{and} \\ [\hat{T}_q + \varepsilon_{fN}(q,Q)]\,|fvN\rangle &= \epsilon^i_{vN}\,|fvN\rangle\end{aligned} \tag{42b}$$

$$\begin{aligned}[\hat{T}_Q + \epsilon^i_{uN}]\,|mN\rangle &= \mathcal{E}_{mN}\,|mN\rangle \quad \text{and} \\ [\hat{T}_Q + \epsilon^f_{vN}]\,|nN\rangle &= \mathcal{E}_{nN}\,|nN\rangle\end{aligned} \tag{42c}$$

where $\hat{T}_q$ and $\hat{T}_Q$ are the kinetic energy operators for the proton and other nuclei, respectively. Within BOA, the total energy of the at fixed N is written as a simple sum of the three contributions:

$$E_{iumN} = \varepsilon_{iN} + \epsilon^i_{uN} + \mathcal{E}_{mN} \tag{43}$$

and similarly for the final diabatic state.

The SHS treatment of PCET rates is valid for reactions ranging from vibronically non-adiabatic to vibronically adiabatic scenarios[126] and rate expressions for various well-defined limits have been achieved. The SHS PCET rate theories are derived following a path analogous to the derivation of ET rates and extension to the GCE is rather straightforward. As done by SHS, the Golden rule formulation is used. Then, the PCET rate constant is written as

$$\begin{aligned}k_{GCE-PCET} &= \frac{2\pi}{\sim\Xi_i} \sum_{N,u,v,m,n} e^{-\beta(E_{iumN}-\mu N)} \left| \langle Nnvf|\hat{V}_N|iumN\rangle \right|^2 \delta(E_{iumN} - E_{fvnN}) \\ &= \frac{2\pi}{\sim} \sum_N \sum_{u,v} \sum_{m,n} p_{iumN} \left| \langle Nnvf|\hat{V}_N|iumN\rangle \right|^2 \delta(E_{iumN} - E_{fvnN})\end{aligned} \tag{44}$$

The obtained form is analogous to the GCE-ET theory developed herein and shares the structure of the canonical PCET rate of SHS. As assumed for ET part, it is expected that the vibrational part of the system does not depend on the number of particles. However, no such assumption is made for the transferring proton *i.e.* the proton potential depends on the charge state. This is written as

$$\Xi_i = \sum_{N,u,m} e^{-\beta(E_{iumN}-\mu N)} \approx Q_m \sum_{N,u} e^{-\beta(\varepsilon_{iN}+\epsilon_{iuN}-\mu N)} = Q_m \Xi_{iu} \tag{45}$$

At this point it is important to stress that the vibronic coupling depends sensitively on the proton donor-acceptor distance R which is included in the rate expression. It is assumed that the coupling can be decomposed as

$$\langle Nnvf|\hat{V}(R)_N|iumN\rangle \approx \langle Nvf|\hat{V}(R)_N|iuN\rangle_q \langle Nn|mN\rangle_Q = V(R)^N_{uv} S^N_{nm} \tag{46}$$

Inserting these two approximations result in PCET rate constant of the form

$$\begin{aligned} k_{GCE-PCET} &\approx \frac{2\pi}{\sim} \sum_{N,u,v} \frac{e^{-\beta(\varepsilon_{iN}+\epsilon_{iuN}-\mu N)}}{\Xi_{iu}} \sum_{m,n} \frac{e^{-\beta \mathcal{E}_{mN}}}{Q_m} \left|V(R)^N_{uv}\right|^2 \left|S^N_{mn}\right|^2 \delta(E_{iumN} - E_{fvnN}) \\ &= \frac{2\pi}{\sim} \sum_{N,u,v} p_{iuN} \sum_{m,n} p_m \left|V(R)^N_{uv}\right|^2 \left|S^N_{mn}\right|^2 \delta(E_{iumN} - E_{fvnN}) \end{aligned} \tag{47}$$

This form is amenable to the direct treatment as performed by SHS. Depending on the treatment of the R coordinate, several appropriate limits may be considered each yielding a different canonical rate constant. The derivations for the R-dependent PCET rates follow a similar (but more complex [55]) cumulant expansion as performed above for ET. Hence, the GCE-PCET rate can be obtained by extending the approach presented above for the ET. The extension of PCET in GCE is straight-forward and here I present only the most simple result valid under the same conditions as the Marcus-like expression derived above for ET. Specifically, one assumes that[127] i)the short time approximation of the energy gap correlation is valid, ii) high-temperature limit is taken, and iii) that the R coordinate is static giving

$$k = \sum_{N,u} p_{iu} \sum_v \frac{\left|V(R)^N_{uv}\right|^2}{\sim\sqrt{4\pi k_{\mathrm{B}} T \lambda_{uv}}} \exp\left[-\frac{\left(\Delta E^N_{uv} + \lambda_{uv}\right)^2}{4 k_{\mathrm{B}} T \lambda_{uv}}\right] \tag{48}$$

where the reaction energy between vibrational states iuN and fvN is $E^N_{uv} = E_{fvnN}(q_F, Q_F) - E_{iumN}(q_I, Q_I)$. The state-dependent reorganization energy $\lambda_{uv} = E_{ium}(q_F, Q_F) - E_{fvn}(q_F, Q_F)$ is assumed independent of the particle number. If some vibrational modes (besides the R mode) are sensitive to changes in the particle number, they can be separated from the total reorganization energy by decomposing the total reorganization energy

to inner- and outer-sphere components as shown in Appendix H. Depending on the form of the prefactor, both electronically and vibronically adiabatic and non-adiabatic limits of PCET can be reached within the semiclassical treatment[22, 128, 129] of the prefactor.

4.3. Analysis of the non-adiabatic GCE rates

The main difficulty observed in the GCE non-adiabatic rate theory is the treatment of the electronic/vibronic coupling constant; this term is defined only for particle conserving transitions. This precludes the straightforward use of GCE diabatic states which have different number of electrons at the same geometry. Only at the thermodynamic limit when the particle number fluctuation is zero can the GCE diabatic states be used for computing the coupling constant. However, at this limit the GCE-NATST is equal to the canonical NATST as only a single particle number state is populated i.e. p_i becomes a delta function around some particle number. At thermodynamic limit either using fixed potential GCE states or fixed particle number canonical states will give equivalent results as they should.

Even at the thermodynamic limit the present treatment differs from the traditional Dogonadze-Kutzetnotsov-Levich[50]. Schmikler-Newns-Anderson[51, 52], and SHS approaches. A detailed discussion is given in the Appendix A and here only the main differences are high-lighted. The crucial difference is that the present formulation does not rely on the separation of the total interacting wave function to non-interacting or weakly interacting fragments. In the present approach, the applied electrode potential does not only affect the electrode alone but rather modifies the entire systems affecting all electrode, reagent, and solvent species. Hence, the inherent complexity of the electrochemical interface is naturally included in the Hamiltonian and the wave function from the start. Another crucial difference is that the charge transfer kinetics are not decomposed into single electron orbital contributions. Instead, the work herein formulates the kinetics in terms of many-body diabatic wave functions. In the canonical ensemble, such an approach has been shown[130] to provide accurate barriers, prefactors, and overall kinetics for electron transfer reaction in battery materials.

For small systems where particle number fluctuations are pronounced the summation over particle numbers need to be performed. While straightforward in principle, the amount of calculations can seem daunting at first. However, as the populations depend exponentially on the energy and target chemical potential, $p_{iN} \sim \exp[-\beta(E_{iN} - \mu N)]$, only a limited number of

states will contribute to the summation. In the Appendix F, it is shown that for graphene, the electrode potential around the PZC±0.5V is accurately captured using seven different charge states. It is expected that the infinite summation can be safely reduced to summation over a small number (5–10) of different charge states covering the electrode potential range of interest. Again, at the thermodynamic limit only a single calculation *per* potential is needed.

For practical applications interpolation between adiabatic and non-adiabatic regions is often needed. The most commonly utilized way to achieve this in the canonical ensemble is to use the Landau-Zener interpolation formula (see *e.g.* Ref. 100). A similar interpolation can performed also within the GCE in two ways – for the fixed number states or the effective fixed potential. In the former, the Landau-Zener prefactor is computed for each charge state and utilized in the summation. In the latter one replaces the particle number dependent prefactor with an effective or averaged prefactor as in Eqs.(7) or (C.6). At the thermodynamic limit both will be equivalent. Investigating this interpolation for smaller systems is not within the scope of the present work and is left for future studies.

5. Conclusions

This work presents a general rate theory for open systems. If only the electronic subsystem is open, the formulation yields electrochemical and electrocatalytic rates at fixed electrode potentials. The rate equations are derived by extending the canonical rate theory[61–63] to the grand canonical, fixed potential ensemble. It is shown that all rate theories developed within the canonical ensemble can be extended to GCE. Specifically, ways to address e.g. adiabatic, non-adiabatic, and tunnelling reactions can be formulated within GCE. In this work, the grand canonical formulation is applied to derive rate constants for i) general electrocatalytic reactions with (Eq. (8)) and without (Eq. (2)) the TST approximation, ii) adiabatic ET and PCET reactions using a grand canonical Marcus-like EVB theory in Eq. (18) , and iii) non-adiabatic ET in Eq. (40) and PCET in Eq. (48). Future work will provide interpolation between the derived adiabatic and non-adiabatic rate equations. To summarize, the theoretical work presented herein provides a unified framework for computing and understanding both inner-sphere (electrocatalytic) and outer-sphere (electrochemical) reaction kinetics as a function of the electrode potential.

In its most general form, the fixed potential rate theory requires computation of canonical rates for a set of systems with a varying number of electrons (and/or nuclei). Summing and weighting the different canonical ensemble rates can be relaxed if one assumes that the prefactor or transmission coefficient is independent on the number of particles in the system. Assuming a constant transmission coefficient directly leads to TST like equations (Eqs. (7) and (8)) where the reaction rate depends exponentially on the grand energy barrier $\Delta\Omega^{\ddagger}$. This is most useful and provides the theoretical basis for computing adiabatic reaction rates within GCE-TST as done in several recent publications[12, 19, 20, 35, 36, 131, 132] in which the rate expression was used without *a priori* justifying the use of such rate equations.

Further insight in the (adiabatic) reaction rates and energy barriers is obtained from a Marcus-like, grand canonical ensemble empirical valence bond (GCE-EVB) theory developed in the present work. As shown in Section 3, the GCE-EVB formulation enables writing the grand energy barrier in terms of fixed potential reorganization energy and the reaction grand energy in analogy with the canonical EVB or Marcus theory. As discussed in Section 3.2, this formulation enables computation and rationalization of both non-linear grand energy relationships and Tafel slopes. Together these may called BEP-Tafel relations. Both can be derived, analyzed and computed using just a few parameters which can be obtained using *e.g.* a combination of fixed potential and constrained DFTs. Based on the BEP-Tafel relationships one determine how the reaction barrier changes as a function of the reaction energy as shown in Figure 3.2. The derived adiabatic GCE-EVB rate, barrier and generalized BEP-Tafel energy relation predict and explain the "Marcus-like" behavior in energy barriers as a function of the thermodynamic driving force observed in recent computational work[20, 36, 38].

To go beyond TST, fixed potential rate constants are derived also for electronically (and vibronically) non-adiabatic ET and PCET reactions. Thus far computational work on non-adiabatic effects and pure ET have remained scarce despite their practical importance in providing new reaction pathways to avoid constraining scaling relations[133–135] encountered for adiabatic PCET reactions while predicting catalytic activity as well as in understanding fundamental phenomena in electrocatalysis. As discussed by Schmickler *et.al* in Ref. [136], the absence of computational studies on pure ET in electrocatalytic systems is due to insufficient theoretical and computational methods. The NA-ET rate constants derived herein will especially useful for studying NA effects in outer-sphere ET of electrocatalytic systems. This pro-

vides means to obtain atomic-level insight on pure ET reactions which have remained elusive and neglected in computational studies but have often been observed experimentally, especially on weakly-binding catalysts, as discussed in Section 1. The fixed potential PCET rate equations facilitate the study of kinetics of ubiquitous proton-coupled electron transer reactions. As formulated herein, the PCET rate constant naturally includes both electronic and vibronic non-adiabaticity as well as hydrogen tunneling. This again enables detailed theoretical and computational studies of these experimentally observed, but thus far computationally largely neglected, electrocatalytic reactions.

All the rate equations derived in this work can be directly utilized and combined with general Hamiltonians used in *e.g.* electronic DFT. For non-adiabatic kinetics and GCE-EVB, methodology for computing diabatic curves is needed; constrained DFT[95–97] implemented in various DFT codes[137–147] is ideally suited for this and facilitates adopting the rate equations derived herein. TST-like rate equations can be computed using energies from grand canonical DFT which is also currently available in several codes in various forms[3, 10–20].

Combining the presented rate theory with currently existing DFT methods and various solvation models is straight-forward and enables the study of electrochemical and electrocatalytic kinetics at realistic electrochemical interfaces. This will greatly improve our microscopic understanding by enabling computation of electrocatalytic kinetics as a function of the electrode potential and addressing tunneling and non-adiabaticity in electrocatalysis. Hence, a wide variety of mechanistic, kinetic and thermodynamic aspects of electrocatalytic reactions can be addressed on equal footing within GCE and the complex interplay between the electrode potential, solvation, double-layer and electrocatalysis can be studied from first principles. Besides providing a rigorous and general theoretical framework for fixed potential kinetics, the advances herein enable computational studies on pure ET and PCET with hydrogen tunnelling pathways to circumvent scaling relations often encountered in electrocatalysis.

6. Acknowledgements

I acknowledge support by the Alfred Kordelin Foundation and the Academy of Finland (Project No. 307853). I also thank Professor Sharon Hammes-Schiffer, Dr. Alexander Soudackov, Dr. Yan Choi Lam, and Mr. Zachary

Goldsmith for hosting my visit to the Hammes-Schiffer group at Yale, for the useful discussions and help on formulating the ET and PCET rates within the grand canonical ensemble. Computational resources were provided by CSC IT CENTER FOR SCIENCE LTD.

7. Declaration of interest

Declarations of interest: none

Appendix A. Problem for choosing filled and empty orbitals in "orbital-based" rate theories

Appendix A.1. Orbital based electron transfer rate theories

There are two commonly used orbital based approaches for writing the charge transfer rate at an electrode surface. The first one was developed by Dogonadze, Levich, and Kutznetsov (DLK)[49], who assumed a weak interaction between the donor and acceptor. Their treatment yields an expression similar to Marcus theory and the model is often called Marcus-Hush-Chidsey[120], Gerischer[148], Marcus-DOS[148] or just the density-of-states (DOS) model. In the case of a metallic electrode, the molecular orbital will interact with a continuum of electronic states from the metal and therefore one needs to integrate over all the metallic bands. An implicit assumption in the DOS model is that charge transfer takes place between two one-electron orbitals rather than two many-electron wave functions. Also, the effect of the electrode potential E is assumed to linearly shift the energy of the initial state without changing the one-electron levels. For electrochemical charge transfer reactions the DOS equation written in terms of a molecular orbital ϵ_0 and its DOS $\rho_0(\epsilon_0)$ and (quasi-continuum) of electrode bands ϵ with DOS $\rho(\epsilon)$. In this case the charge transfer is [49, 50] (see also Appendix A)

$$k_{DOS}(E) = \int d\epsilon W(\epsilon, \epsilon_0) f(\epsilon - E) \rho(\epsilon) \rho_0(\epsilon_0) \tag{A.1}$$

where W is the transition probability and f is the Fermi-Dirac distribution. Originally, the DLK model was derived for the weak interaction limit and harmonic energy surfaces results in the well-known equation [49, 50]

$$k_{DOS}(E) \approx \sqrt{\frac{\beta}{4\pi\lambda}} \int_{-\infty}^{\infty} d\epsilon |H_{ab}(\epsilon, \epsilon_0)|^2 f(\epsilon - E) \exp\left[-\beta \frac{(\lambda + e_0(E^0 - E) - \epsilon_0)^2}{4\lambda}\right] \tag{A.2}$$

$H_{ab}(\epsilon, \epsilon_0) = \langle \psi_a^{\epsilon_0} | \hat{H} | \psi_b^{\epsilon} \rangle$ denoting the Hamiltonian matrix element between the molecule and electrode orbitals corresponding to energy levels ϵ_0 and ϵ, respectively, in the initial a and final b diabatic states. E is the electrode potential and E^0 is the formal equilibrium potential. Depending on the model used for the reactant DOS, the weakly interacting limit by Dogonadze, Gerischer's model with a Gaussian dependency or Schmickler's model (see below) maybe obtained as shown in Ref. 149

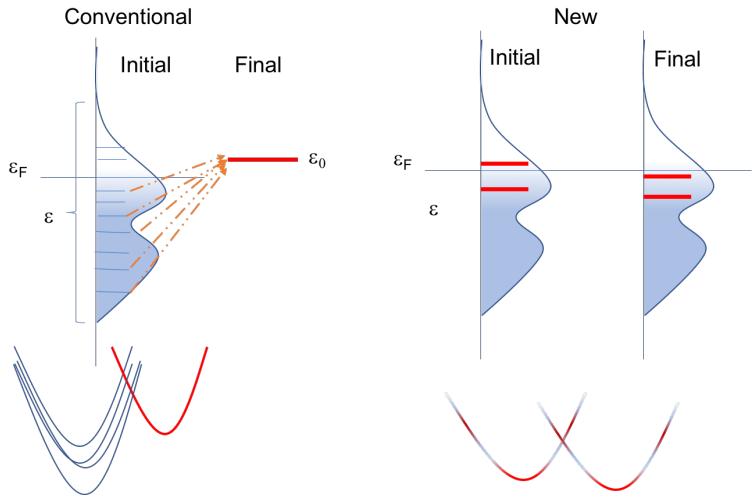

Figure A.4: Conventional (left) and GCE Marcus theory (right). The conventional theory is based on transitions between single-electron orbitals while the current GCE framework utilized general many-electron wave functions.

The other approach is due to Schmickler[51, 52] and has been dubbed as the potential energy curve (PEC) method. The PEC method applies a modified Newns-Anderson (N-A) Hamiltonian for building potential energy surface (pes)

$$H_{N-A} = \epsilon_0 n_0 + \sum_k \epsilon_k n_k + \sum_k (v_{k0} c_k^\dagger c_r + v_{rk} c_0^\dagger c_k) + \frac{1}{2} \sum_i \sim\omega_i (p_i^2 + q_i^2) + (n_0 - z) \sum_i (\sim\omega_i g_i q_i) \tag{A.3}$$

where the terms describe reactant orbital, orbitals of the electrode, electron exchange terms using coupling matrix elements v, harmonic bath at frequencies ω_i, momenta p_i and coordinate q_i while the last term couples the reactant at charge state z to the harmonic bath. Connecting the initial and final states of the redox reaction along a charge transfer coordinate r_q and using N-A Hamiltonian, the PES is

$$u(r_q, \epsilon_F) = \frac{r_q^2}{4\lambda} + (\epsilon_0 + r_q - \epsilon_F)\langle n(r_q)\rangle + \frac{\Delta}{2\pi} \ln[(\epsilon_F - r_q - \epsilon_0) + \Delta^2] \tag{A.4}$$

where $\langle n(r_q)\rangle = 1/2 + 1/\pi \tan^{-1}((\epsilon_F - r_q - \epsilon_0)/\Delta)$ is the charge at r_q and $\Delta(\epsilon') = \pi \sum_k |v_{0,k}|^2 \delta(\epsilon' - \epsilon_k)$ is the effective coupling constant. Then, the charge transfer barrier is $u^\ddagger = u(r_q = r_{max}, \epsilon_F) - u(r_q = 0, \epsilon_F)$ and the rate is

$$k_{PEC} = \kappa \exp\left[-\beta u^\ddagger\right] \tag{A.5}$$

At the weak interaction limit, both the DOS and PEC models are in their essence formulations of Fermi's Golden rule describing electron transfer between single electron orbitals.

Appendix A.2. Orbital based Fermi Golden rule formulation

If initial (final) state at the initial (final) geometry can be approximated by a single diabatic electronic state $\Psi(R_{initial}) \approx |\psi_I\rangle\,|\chi_j\rangle$, the Hamiltonian in Eq.(A.6) leading to Fermi's golden rule as follows. A similar equation can also be written for adiabatic states as shown in Ref. 93, 94. In the diabatic Fermi Golden rule formulation the Hamiltonian is [62, 72]

$$\begin{aligned}\hat{H}_{el} = &\sum_i E_i^I \left|I^i\right\rangle \left\langle I^i\right| + \sum_f E_f^F \left|F^f\right\rangle \left\langle F^f\right| \\ &+ \sum_{if} \Delta_{if}(\left|I^i\right\rangle \left\langle F^f\right| + \left|F^f\right\rangle \left\langle I^f\right|)\end{aligned} \tag{A.6}$$

where $\left|K^k\right\rangle = |\psi_k\rangle |\chi_k\rangle$ is a vibronic wave function consisting of $|\psi_k\rangle$, a one electron orbital and $|\chi_j\rangle$ a nuclear wave function. Reaction rates using this diabatic Hamiltonian is achieved using the general flux formulation presented in the main article with the following transition probability and flux[62, 72]: $P(E) = \frac{1}{2}(2\pi\sim)^2 \operatorname{Tr}\left[\hat{F}\delta(E-\hat{H}_N)\hat{F}\delta(E-\hat{H}_N)\right]$ and $\hat{F} = 1/\sim\Delta[|0\rangle\langle 1| + |1\rangle\langle 0|]$, respectively. Δ_{if} is a general diabatic coupling term, which in the Franck-Condon approximation is

$$\begin{aligned}\Delta_{if} &= \left|\langle\psi_f|\hat{V}|\psi_i\rangle\right|^2 \sum_{kl} |\langle\chi_k|\chi_l\rangle|^2 \\ &= |V_{if}|^2 \sum_{kl} |\langle\chi_k|\chi_l\rangle|^2\end{aligned} \tag{A.7}$$

Following standard thermalized Fermi-golden rule derivation[62, 72, 101] for a transition between two electronic states gives

$$k_{I\to F} = \frac{2\pi}{\sim} \sum_{i\in I, f\in F} k_{i\to f} \tag{A.8a}$$

$$\begin{aligned}k_{i\to f} &= \frac{|V_{if}|^2}{\sum_l \exp[-E_{i,l}]} \sum_{lk} \exp[-E_{i,l}]|\langle\chi_k|\chi_l\rangle|^2 \times \delta(E_i - E_f + E_l - E_k) \\ &= |V_{if}|^2 F(E_i - E_f)\end{aligned} \tag{A.8b}$$

where $F(E_i - E_f)$ is the thermally averaged Franck-Condon factor. If the nuclear wave functions are taken to be those of a harmonic oscillator, the Marcus barrier and the rate constant can be obtained from the derivation in Appendix C. Note that transition between all one electron orbitals are considered here.

To obtain the DOS-model for electron transfer, only a subset of the transition rates is considered. Intuitively, for an reduction of a molecule, transitions from the localized occupied metal orbitals to empty orbitals localized at the molecule should be considered. This leads to

$$\begin{aligned} k_{red} &= \frac{2\pi}{\sim} \sum_{i \in \text{filled}} \sum_{f \in \text{empty}} k_{i \to f} \\ &= \frac{2\pi}{\sim} \sum_{f \in \text{empty}} \int d\epsilon_i \rho(\epsilon) f(\epsilon - \epsilon_F) k_{i \to f} \end{aligned} \tag{A.9}$$

where the second equation highlights the close correspondence with the DOS method (Eq. (A.1)), $\rho(\epsilon)$ is the DOS and f the Fermi-Dirac distribution. Note also that the PEC method uses a Hamiltonian similar diabatic Hamiltonian here. In PEC the total transition probabilities from initial to final state are also computed using orbital-to-orbital formulation described above.

Appendix A.3. Choosing the orbitals

Both DOS and PEC share a fundamental open question: how does one choose the localized and empty/filled orbitals? This situation is faced in a typical first-principles calculations, where (canonical) one electron orbitals are highly delocalized even when charge-localized diabatic states are used, making the choice of active orbitals difficult. An important result learned from orbital localization methods[150–153] is that the energy from a single determinant method such as DFT or Hartree-Fock methods is invariant to orbital rotation within the *occupied molecular orbitals*. Thus, occupied orbitals can be localized using a unitary rotation which leaves *the energy, and the total wave function unchanged*; during this process the spatial shape and spread of filled one electron orbitals are drastically changed. Also, the empty, virtual orbitals can be localized separately. However, the filled and empty are not allowed to mix during the localization to avoid changes in occupation of numbers[154]. As mixing is forbidden, orbital localization is performed separately for the empty and filled orbitals and consequently two different unitary transforms are required.

A concrete example helps to understand why the orbital localization cause practical difficulties. Consider for example an outer-sphere ET from an electrode to O_2 forming a superoxide species. Here the initial state wave functions

$\{|I\rangle\}$ would be occupied orbitals localized on the metal and the final state orbitals $\{|F\rangle\}$ would be empty states localized on O_2. After a normal DFT calculation, one performs a unitary transform on both the initial and final states separately such that the the orbitals are well localized to the molecule and metal for both states: $|I\rangle = \hat{U}\left|I_{DFT}^{filled}\right\rangle$ and $|F\rangle = \hat{V}\left|F_{DFT}^{empty}\right\rangle$, with $\hat{U}\hat{U}^\dagger = 1$ and $\hat{V}\hat{V}^\dagger = 1$. Note that nuclear wave function remain unchanged as the electronic energy is unaffected by the transformation. Thus, the unitary transformation leaves the thermally averaged Franck-Condon weight unchanged.

However, the electronic coupling elements for a given $V_{if} = \langle i|\hat{H}|f\rangle$ change drastically as the electronic orbitals are rotated. This is easily seen from the close correspondence[155] between the coupling and overlap elements $\langle i|V|f\rangle \approx v\,\langle i|f\rangle$, where v is a constant. Changing from the localized to delocalized states is written as $\langle i|f\rangle = \langle i_{dft}|\hat{U}^\dagger\hat{V}|f_{dft}\rangle \neq \langle i_{dft}|f_{dft}\rangle$ when final (empty) and initial (filled) canonical DFT orbitals are localized separately. Only when $\hat{U} = \hat{V}$ is the overlap between the localized and canonical orbitals the same; this would require of mixing of the filled and empty canonical orbitals resulting in changes in the total energy and the total wave function and is therefore discouraged.

As a concrete example consider Eq. (A.9) where only states below the Fermi-level contribute to the reduction rate. As potential is changed, some orbitals become empty or occupied changing the driving force of the reaction which remains unchanged under the orbital localization. The rate is dictated by transition probability directly related to the matrix elements in non-adiabatic reactions. *Thus, the rate of non-adiabatic electron transfer reaction depends on how the orbitals are chosen and localized.* This can lead to inconsistent and incorrect interpretation of the electrochemical rate as a function of the potential if basic single determinant methods are used to parametrize the DOS or PEC models. Great care is needed when the methods and as emphisized in Ref. 82 "this is not a failure of the computational methods used but is a consequence of how the rate constant is defined by the phenomenological equations. It is therefore important to choose the approach which is equivalent to the experiment or thought experiment that the theory is attempting to reproduce".

Based on the above discussion, a very important conclusion is reached: the rate obtained from the Fermi golden rule, DOS or PEC using only the "active orbitals" depend on the way the orbitals are localized. Therefore,

one needs to acknowledge that orbital localization needed when the orbital-based models are parametrized using canonical DFT methods, leads to arbitrary changes in the rate constant depending on the localization or rotation used scheme. Hence, while the energy, density, and the total wave function remain unchanged after a unitary transformation of the orbitals, single orbitals and single orbital overlaps will necessarily be affected. Therefore, a unitary transformation such as orbital localization will unphysically affect the rate obtained from methods using one-electron orbitals and orbital-to-orbital transitions to compute the transition probability. If one electron-based the DOS or PEC methods are parametrized using first-principles approaches, methods such as fragment orbital DFT[156] methods might be applicable.

Care is also required when using many-body wave functions for computing the rates. While unitary transform does not change any observables of a single diabatic wave function, the off-diagonal matrix elements might be sensitive to orbital rotations. However, in approaches such constrained DFT employed in this work, the coupling elements are functionals of the electron densities of the initial and final state[96] and as such in principle unaffected by orbital localization.

Appendix B. Grand canonical formulation for electrochemical systems

Below the necessary details for grand canonical formalism are presented. A more complete treatment is given in Ref. 3.

Within GCE all expectation values are computed using

$$\langle O \rangle = \mathrm{Tr}\Big[\hat{\rho}\hat{O}\Big] \tag{B.1}$$

with the grand canonical density operator

$$\hat{\rho} = \frac{\exp\Big[-\beta(\hat{H}_{tot} - \sum_i \tilde{\mu}_i \hat{N}_i)\Big]}{\mathrm{Tr}\left[\exp\Big[-\beta(\hat{H}_{tot} - \sum_i \tilde{\mu}_i \hat{N}_i)\Big]\right]} \tag{B.2}$$

where $\hat{H}_{tot}$ is the Hamiltonian, $\tilde{\mu}_i$ is the electrochemical potential of species i, and $\hat{N}$ is the number operator. The partition function is defined as $\Xi = \mathrm{Tr}\Big[\exp\Big[-\beta(\hat{H}_{tot} - \sum_i \mu_i \hat{N}_i)\Big]\Big]$ from which the grand free energy is

$\Omega[T,V,\mu] = -k_B T \ln \Xi = E - TS - \sum_i \mu_i N_i$. The probability of being in microstate i is

$$p_i^{GC} = \frac{\exp\left[-\beta \left\langle \Psi_i | \hat{H}_{tot} - \sum_j \tilde{\mu}_j \hat{N}_j | \Psi_i \right\rangle\right]}{\Xi} \tag{B.3}$$

In the above equation, $|\Psi_i\rangle$ is the total wave function of both the electrons and nuclei so that the particle number operators $\hat{N}_i$ corresponds to electrons or the nuclear identities as specified below. With these definitions fixed potential, grand canonical can be computed. For example, the grand energy for electrons n and electrolyte $\pm$ with fixed chemical potential is is given by

$$\begin{aligned}\Omega(T,V,\tilde{\mu}_\pm,\tilde{\mu}_n) &\equiv \sum_i p_i \left[\beta \ln p_i + \left\langle \Psi_i | \hat{H}_{tot} - \mu_\pm(\hat{N}_+ + \hat{N}_-) - \tilde{\mu}_n \hat{N}_n | \Psi_i \right\rangle\right] \\ &= \mathrm{Tr}\left[\hat{\rho}\hat{\Omega}\right] \equiv \Omega[\hat{\rho}]\end{aligned} \tag{B.4}$$

Appendix C. Adiabatic and non-adiabatic harmonic TST rates

Here classical harmonic TST (HTST) for adiabatic and non-adiabatic reactions within GCE are derived.

Appendix C.1. Adiabatic HTST

The general TST rate equation is shown in Eq. (7). First, consider a general case where potential the number of both nuclei and electrons is allowed to fluctuate. Usually, for N_N classical nuclei the Hamiltonian in mass-weighted coordinates ($\mathbf{x}_i$) and momenta P_i is written as $H_{cl} = \sum_{i \in N_N} P_i^2 + V(\mathbf{x}_i)$. $V(\mathbf{x}_i)$ defines the (Born-Oppenheimer) potential energy surface.

Then consider a system is open to electrons at a fixed electron chemical potential while number of nuclei is fixed. Also, the system is assumed adiabatic meaning that the number and distribution of electrons adjusts instantaneously to the nuclear configuration. This is the common situation considered in first principles calculations at fixed electrode potential calculations. For this case, the Kohn-Sham-Mermin theorem guarantees that electronic energy and distribution are unique to a given electron chemical potential and external potential (here provided by the nuclei). Hence, the potential energy V is not only a parametric function of the nuclear positions

but also the chemical potential of the electrons. Furthermore, as shown in Ref. 3, the grand free energy of the electrons is given by $\Omega_n(T, V, N_N, \mu_n; \mathbf{x}_i)$. As the nuclei move the on the effective potential energy surface provided by the electrons, one recognizes that $V(\mathbf{x}_i, \mu_n) = \Omega_n(T, V, N_N, \mu_n; \mathbf{x}_i)$ (see Ref. 3 and Appendix B). Then, for the open electronic system, the classical Hamiltonian for the nuclei is

$$H(N_N)_{cl} = \sum_{i \in N_N} P_i^2 + V(\mathbf{x}_i, \mu_n) \equiv H_{cl} \tag{C.1}$$

where I and $\ddagger$ denote the initial and transition states. The TST rate is written as [101]

$$k_{TST}(N_N, V, T)Q_I = \int_N dP \int_N d\mathbf{x} \exp\Big[-H_{cl}^{\ddagger}\beta\Big]\delta(f(\mathbf{x}))(\nabla f \cdot P^N)h(\nabla f \cdot P^N) \tag{C.2}$$

where f is the $N-1$ dimensional dividing surface between the reactants and products, $\nabla f \cdot P^N = P_{n^\ddagger}$ is the momentum normal to f identified as the reaction coordinate, $h(\nabla f \cdot P^N) = h(P_{n^\ddagger})$ is a step function separating the reactant ad product basins, and $\delta(f(x^N))$ restricts the geometries to lie on the dividing surface. With these definitions the canonical HTST at fixed electron chemical potentials follows from:

$$\begin{aligned}
k_{HTST}(T, V, N_N) &= \int_N dP \int_{N-1} d\mathbf{x} P_{n^\ddagger} \frac{\exp\Big[-H_{cl}^{\ddagger}\beta\Big]}{Z_I} \\
&= \frac{\int_N dP \int_{N-1} d\mathbf{x} P_{n^\ddagger} \exp\Big[-\beta(\sum_{i=0}^N 1/2P_i^2 + V(\mathbf{x}_i, \mu_n)^\ddagger)\Big]}{\int_N dP \int_N d\mathbf{x} \exp\Big[-\beta(\sum_{i=0}^N 1/2P_i^2 + V(\mathbf{x}_i, \mu_n)^I)\Big]} \\
&= \frac{1}{\sqrt{2\pi\beta}} \frac{\int_{N-1} d\mathbf{x} \exp\big[-\beta V(\mathbf{x}_i, \mu_n)^\ddagger\big]}{\int_N d\mathbf{x} \exp[-\beta V(\mathbf{x}_i, \mu_n)^I]} \\
&\approx \frac{v_N}{\sqrt{2\pi}} \frac{\prod_i^{N-1} v_i}{\prod_i^{N-1} v_i^\ddagger} \exp\big[-\beta(\Omega_n^\ddagger - \Omega_n^I)\big] \\
&= \frac{v_N}{2\pi} \exp\Big[-\beta(\Omega_N^\ddagger - \Omega_N^I)\Big] = \frac{v_N}{2\pi} \exp\Big[-\Delta\Omega_N^\ddagger\beta\Big]
\end{aligned} \tag{C.3}$$

where at the second last row the effective potentials are Taylor expanded in terms of normal mode coordinates with corresponding frequencies v_i and

v_N is the frequency along the reaction coordinate:$V^{\ddagger/I} = \Omega_N^{\ddagger/I} + 1/2\sum_i v_i q_i^2$. The last equality follows from setting the nuclear vibrational entropy $S_N = k_B \ln\left(\prod_i^{N-1} v_i / \prod_i^{N-1} v_i^{\ddagger}\right)$ and setting the total grand free energy to $\Omega_N = \Omega_n - TS_N$. Here the subscript N reminds that the number of nuclei was kept fixed above. **Note that Eq.** (C.3) **would be used in typical first principles calculations at fixed electrode potentials where the electron chemical potential and number of nuclei are fixed.**

The above treatment can also be extended to treat situations in which both the number of electrons and nuclei are allowed to fluctuate. This is straight-forward and can be obtained by. Inserting Eq. (C.3) in (7) and applying Eq. (8) leads to

$$k_{HTST}(T, V, \mu) = \frac{\langle v_N \rangle_\mu}{2\pi} \exp\left[-\Delta\Omega^{\ddagger}\beta\right] \tag{C.4}$$

where $\langle v_N \rangle_\mu$ is the effective frequency along the reaction coordinate computed using effective fixed potential PESs.

Appendix C.2. Non-adiabatic HTST

Next, non-adiabatic harmonic transition state theory (NA-HTST) approximation to the rate is developed. Unlike for the canonical case, only a fixed number of nuclei is treated. NA-HTST also requires the calculation of matrix elements $H_{AB} = \langle \Psi_A | \hat{H} | \Psi_B \rangle$. These H_{AB}s are defined only when $|\Psi_A\rangle$ and $|\Psi_B\rangle$ have the same number of both electron and nuclei. Also, the adiabatic approximation cannot be used and the electrons do not instantaneously adapt to nuclear positions. Hence, unlike for the adiabatic case, constant electron number $V(x, n)$ rather that constant electron potential $V(x, \mu_n)$ is used. The appropriate Hamiltonian is given by Eq. (A.6), in which $H_{cl} = \sum_{i \in N_N} P_i^2/2m_i + V_i(\mathbf{x}_i)$.

Using this Hamiltonian, assuming a quadratic potential V and applying the Golden rule form the basis for NA-HTST. This derivation can be found in *e.g.* Ref 74. Another path, presented below, is to use the classical transitions state theory using the Landau-Zener transition P_r probability[100, 101] and assuming that the potential energies are quadratic. Then, the following identities are used: The reorganization energy and vibrational frequency along the reaction coordinate are related as $\lambda = 2v_N^2 \Delta q^2 = 2mv_N^2 \Delta x^2$, where Δq and Δx are the geometric differences of the initial and final states in mass weighted and cartesian coordinates states, respectively. The differences of

forces can written as gradient of the two parabolas at the transition state as shown in Ref. 74 to yield $|\Delta F|_{\ddagger} = \lambda/\Delta x$. With these definitions, fixed number (canonical) electronic/nuclear NA-HTST can be derived:

$$
\begin{aligned}
k^{na}_{HTST}(T,V,N_N,N_n) &= \int_N dP \int_{N-1} d\mathbf{x} P_r P_{n^\ddagger} \frac{\exp\left[-H^\ddagger_{cl}\beta\right]}{Z_I} \\
&= \int_N dP \int_{N-1} d\mathbf{x} \left(1 - \exp\left[-\frac{2\pi|H_{IF}|^2}{\sim|P_{n^\ddagger}\nabla_{n^\ddagger}(V_I - V_F)|}\right]\right) P_{n^\ddagger} \frac{\exp\left[-H^\ddagger_{cl}\beta\right]}{Z_I} \\
&\overset{\text{linearize exp}}{\approx} \int_N dP \int_{N-1} d\mathbf{x} \frac{2\pi|H_{IF}|^2}{\sim|P_{n^\ddagger}\nabla_{n^\ddagger}(V_I - V_F)|} P_{n^\ddagger} \frac{\exp\left[-H^\ddagger_{cl}\beta\right]}{Z_I} \\
&\overset{\text{forces}}{=} \int_N dP \int_{N-1} d\mathbf{x} \frac{2\pi|H_{IF}|^2}{\sim P_{n^\ddagger}|\Delta F|} P_{n^\ddagger} \frac{\exp\left[-H^\ddagger_{cl}\beta\right]}{Z_I} \\
&\overset{\text{integrate } P}{=} \frac{2\pi|H_{IF}|^2}{\sim|\Delta F|} \frac{\int_{N-1} d\mathbf{x} \exp\left[-V^\ddagger\beta\right]}{\int_N d\mathbf{x} \exp[-V_I\beta]} \\
&\overset{\text{harmonic TST}}{\approx} \sqrt{2\pi\beta}\frac{|H_{IF}|^2}{\sim|\Delta F|} v_N \frac{\prod_i^{N-1} v_i}{\prod_i^{N-1} v_i^\ddagger} \exp\left[-(E^\ddagger - E_I)\beta\right] \\
&\overset{\text{vib. entropy}}{=} \sqrt{2\pi\beta}\frac{|H_{IF}|^2}{\sim|\Delta F|} v_N \exp\left[-\Delta A^\ddagger\beta\right] \\
&\overset{|\Delta F|_\ddagger = \lambda/\Delta x}{\approx} \sqrt{2\pi\beta}\frac{\sqrt{m}v_N\Delta x|H_{IF}|^2}{\sim\lambda} \exp\left[-\Delta A^\ddagger\beta\right] \\
&\overset{\lambda = 2mv_N^2\Delta x^2}{=} \sqrt{\frac{\pi\beta}{\sim^2\lambda}}|H_{IF}|^2 \exp\left[-\Delta A^\ddagger\beta\right] \\
&\overset{\text{Marcus barrier}}{\approx} \sqrt{\frac{\pi\beta}{\sim^2\lambda}}|H_{IF}|^2 \exp\left[-\beta\frac{(\Delta A^0 + \lambda)^2}{4\lambda}\right]
\end{aligned}
\tag{C.5}
$$

The above rate is derived for fixed number of electrons and nuclei. As done for the adiabatic case, this fixed particle rate needs to be turned to a fixed potential rate. In particular, the electronic subsystem needs to be open in order to study kinetics at a fixed electrode potential. However, generalization of the NA-HTST to GCE is significantly more difficult compared the the adiabatic as discussed. The electronically GCE NA-HTST can be accomplished the approach in Section 4 resulting in Eqs. (40) and (48).

To gain more insight, it is useful to compare the above derivation to the GCE-EVB picture used for deriving the GCE equivalent of Marcus barriers i.e. Eq. (18). Using Eq. (8) with the GCE Marcus barrier of Eq. (18) with an effective non-adiabaticity correction gives

$$k_{HTST}^{na}(T,V,N_N,\mu_n) \approx \left\langle \sqrt{\frac{\pi\beta}{\sim^2\lambda}}|H_{IF}|^2 \right\rangle_{\mu_n} \exp\left[-\beta\frac{(\Delta\Omega_{FI}+\Lambda)^2}{4\Lambda}\right] \quad \text{(C.6)}$$

where the prefactor is computed for either i) some particle number and assumed to independent of the electrode potential or ii) various particle numbers and weighted according to the grand canonical distribution.

Appendix D. Grand canonical perturbation theory

If only the electronic subsystem is open, the easiest approach is to use an effective fixed electrode potential Hamiltonian like the one introduced in Eq. (C.1). Then, one solves equations similar to (10) using this effective constant potential Hamiltonian to obtain fixed (electrode) potential diabatic states. Then, the diabatic states and grand energy curves are computed along the reaction coordinate. From the curve crossing point an estimate for the constant (electrode) potential grand energy barrier is obtained.

To keep the present work as general as possible *i.e.* allowing both the number of electron and nuclear species to fluctuate, a simple effective Hamiltonian cannot be specified. Instead, explicitly sampling the GCE and number of electrons and nuclei is needed. In this case, one can follow and extend the general thermodynamic perturbation theory of Zwanzig[104] to GCE. Along these lines, the canonical energy operator $H = H_0 + V$ is defined and partitioned to contributions from the unperturbed H_0 part and a perturbation V. The total GC partition function Ξ and grand energy Ω are given by (see Appendix B)

$$\Xi = \mathrm{Tr}[H - TS - \mu N] \quad \text{and} \quad \exp[-\beta\Omega] = \Xi \quad \text{(D.1)}$$

Then, the total grand energy can be multiplied and divided by the unperturbed grand energy

$$\exp[-\beta\Omega] = \frac{\exp[-\beta(\Omega-\Omega_0)]}{\exp[-\beta\Omega_0]} = \frac{\exp[-\beta(\Omega_V)]}{\exp[-\beta\Omega_0]} = \langle\exp[-\beta V]\rangle_0 \quad \text{(D.2)}$$

where the last identity means that the perturbation part of the grand energy is obtained by performing an GCE sampling of the perturbation part. For electron transfer reactions, the total Hamiltonian can be written as[157]

$$H = K + U + V_x \tag{D.3}$$

where K is the kinetic energy, U is the interaction energy and V_x is the pertubation which depends on extent of the reaction: $x = 0$ and $x = 1$ correspond to initial and final states, respectively. A linear switch from the initial to the final state is obtained by $V_x = V_I - x(V_F - V_I)$. This potential defines the initial and final diabatic states and based on the energies of the initial and final states E_I and E_F, one defines the instantaneous energy gap $\Delta E(R) = E_F(R) - E_I(R) = X$ at geometry R. As noted by Zusman[98] and Warshel[99] (see also Ref. 158 for a combined discussion), the energy gap coordinate is directly related to the (solvent/bath) reorganization coordinate and both are often used in deriving electron transfer rates. It was recently shown by Jeanmairet *et.al.*[157] that the energy gap coordinate is a valid reaction coordinate also within GCE.

Combining the two state GCE diabatic model for the initial I and final F states with the general perturbation result, one obtains,

$$\begin{aligned} \exp[-\beta\Delta\Omega] &= \frac{\langle \exp[-\beta V_F] \rangle_F}{\langle \exp[-\beta V_I] \rangle_I} \\ &= \frac{\sum_N e^{\beta\mu N} \int dP^N dR^N e^{-\beta V_F}}{\sum_N e^{\beta\mu N} \int dP^N dR^N e^{-\beta V_I}} = \frac{\Xi_F^V}{\Xi_I^V} \end{aligned} \tag{D.4}$$

which gives $\Delta\Omega = -\beta^{-1} \ln\left(\Xi_F^V / \Xi_I^V\right)$. Next, the sampling is constrained to a specific region of the energy gap. As recently shown in Ref. 157, a one-to-one mapping exists between the vertical energy gap $\langle \Delta E \rangle_x$, x, the potential V_x, and the probability (p_x) of being in microstate sampled from the GCE: $x \leftrightarrow \langle \Delta E \rangle_x \leftrightarrow V_x \leftrightarrow p_x$. Introducing the energy gap coordinate and noting that the energies of I and F are computed from the same Hamiltonians except for the "perturbation" part, allows writing

$$\begin{aligned} \Delta\Omega = -\beta^{-1} \ln\left(\frac{\sum_N e^{\beta\mu N} \int dP^N dR^N e^{-\beta(\Delta E + V^I)}}{\sum_N e^{\beta\mu N} \int dP^N dR^N e^{-\beta V^I}} \right) = \\ -\beta^{-1} \ln \left\langle e^{-\beta\Delta E} \right\rangle_I = \beta^{-1} \ln \left\langle e^{\beta\Delta E} \right\rangle_F \end{aligned} \tag{D.5}$$

where $\Delta E = V_F - V_I$ is used. One can also obtain a probability distribution for the energy gap by performing constrained sampling[101] of the grand energy curves

$$\bar{\Xi}^i(X) = \sum_N e^{\beta\mu N} \int dP^N dR^N e^{-\beta E_i} \delta(\Delta E(R) - X) \tag{D.6a}$$

$$p^i(X) = \frac{\bar{\Xi}^i(X(R))}{\Xi^i} = \langle \delta(\Delta E(R) - X) \rangle_i = \frac{\sum_N e^{\beta\mu N} \int dR^N dP^N \delta(\Delta E(R) - X) e^{-\beta E_i}}{\sum_N e^{\beta\mu N} \int dR^N dP^N e^{-\beta E_i}} \tag{D.6b}$$

so that $\Xi^i = \int dX \bar{\Xi}^i(X) \equiv e^{-\beta\Omega_i}$ and $\Omega^i(X) = -\beta^{-1} \ln(p^i(X)) + \Omega^i$. Above Ω^i is the diabatic grand energy and $i = I$ or F. Using the last identity and observing that integration over the probability is unity, leads to

$$\Omega^i = -\beta^{-1} \ln \int dX e^{-\beta\Omega^i(X)} \tag{D.7}$$

To arrive at an important identity linking the diabatic grand energies to the energy gap is obtained by using the energy gap as the reaction coordinate X after writing

$$\begin{aligned}
\bar{\Omega}_I(\Delta E) &= -\beta^{-1} \ln\big(\bar{\Xi}_I(\Delta E)\big) = \\
&- \beta^{-1} \ln\left(\sum_N e^{\beta\mu N} \int dP^N dR^N e^{-\beta E_I(R^N)} \delta(\Delta E(R^N) - \Delta E) \right) \\
&= -\beta^{-1} \ln\left(\sum_N e^{\beta\mu N} \int dP^N dR^N e^{-\beta(E_F(R^N) - \Delta E(R))} \delta(\Delta E(R^N) - \Delta E) \right) \\
&= -\beta^{-1} \ln\left(e^{\beta\Delta E} \sum_N e^{\beta\mu N} \int dP^N dR^N e^{-\beta(E_F(R^N))} \delta(\Delta E(R^N) - \Delta E) \right) \\
&= -\Delta E - \beta^{-1} \ln\left(\sum_N e^{\beta\mu N} \int dP^N dR^N e^{-\beta E_F(R^N)} \delta(\Delta E(R^N) - \Delta E) \right) \\
&= -\Delta E + \bar{\Omega}_F(\Delta E)
\end{aligned} \tag{D.8}$$

At this point all relevant free energy identities within the GCE corresponding to the commonly used identities used for deriving the canonical

Marcus theory have been derived.[99, 105–110] Refs. 99, 105–110 show various ways to obtain the iconic canonical Marcus rate constant. To arrive at the corresponding rate constant in the GCE, it is shown that detailed balance is satisfied. At the transition state the initial and final diabatic grand energies are equal giving

$$\begin{aligned}
&\Omega_I(\Delta E^\ddagger) = \Omega_F(\Delta E^\ddagger) \\
&\quad \rightarrow -\beta^{-1}\ln\big(p_I(\Delta E^\ddagger)\big) + \Omega_I = -\beta^{-1}\ln\big(p_F(\Delta E^\ddagger)\big) + \Omega_F \\
&\quad \rightarrow \frac{p_I(\Delta E^\ddagger)}{p_F(\Delta E^\ddagger)} = \exp[-\beta(\Omega_F - \Omega_I)] = \exp[-\beta\Delta\Omega_{FI}]
\end{aligned} \tag{D.9}$$

which shows that detailed balance is satisfied. The diabatic grand energy surfaces are computed from the energy gap distribution[109]

$$\begin{aligned}
g_I(\Delta E) &= -\beta^{-1}\ln(p_I(\Delta E)) \quad \text{and} \\
g_F(\Delta E) &= -\beta^{-1}\ln(p_F(\Delta E)) + \Delta\Omega_{FI}
\end{aligned} \tag{D.10}$$

The transition state can then be identified from the intersection of the relatice grand energy curcves: $g_I(\Delta E^\ddagger) = g_F(\Delta E^\ddagger)$. Computing the reaction rate using the standard transition state theory expression gives

$$k_{IF} = \kappa\frac{\exp\big[-\beta g_I(\Delta E^\ddagger)\big]}{\int d\Delta E\exp[-\beta g_I(\Delta E)]} = \kappa p_I(\Delta E^\ddagger) \tag{D.11}$$

showing that the reaction rate is determined by the energy gap distribution function $p^I(\Delta E) = \langle\delta(\Delta E(R) - \Delta E)\rangle_I$ from Eq. (D.6). Note, that microscopic reversibility is satisfied by construction. To obtain the iconic Marcus rate within GCE, one may follow the perturbation theory route[104, 109] and perform a cumulant expansion on the energy gap distribution as was done also when deriving the GCE-NATST in this work in section 4. It has been shown in several previous studies[106, 109, 121] that the second order cumulant expansion results a Gaussian form for the energy gap distribution

$$p_I(\Delta E) = \frac{1}{\sqrt{2\pi\sigma_I}}\exp\left[-\frac{(\Delta E - \langle\Delta E\rangle_I)^2}{2\sigma_I^2}\right] \tag{D.12}$$

where $\langle\Delta E\rangle_I$ is the energy gap expectation value in the initial state obtained from Eq. (D.6) and $\sigma_I = \langle(\Delta E)^2\rangle_I - (\langle\Delta E\rangle_I)^2$ is the gap variance.

The Marcus relation is then obtain after standard manipulations[100, 106] by inserting these relations in Eq. (D.8) result in the GCE Marcus rate of Eq. (18)

Appendix E. Thermodynamic analysis of outer-sphere ET in macroscopic systems

Consider a general outer-sphere ET reaction $e^-(M) + B(sol) \leftrightharpoons B^-(sol)$ where an electron is transferred from the metal (M) to molecule B in the solution phase (sol). The equilibrium potential is E^{eq}. Changing the potential from E_{eq} to E i.e. introducing the over-potential $\eta = E - E^{eq}$ changes the electron energy by $\Delta\mu_e = -\eta$ for the initial state. The energy of the final state changes as $\Delta\mu^{sol}_{B^-} = -F\Delta\phi_{sol}(\eta)$ where ϕ_{sol} is the electrostatic potential in the solution phase. The reaction energy is changed by $\Delta A = -[\Delta\phi_{sol}(\eta) - \eta]$. $\Delta\phi_{sol}(\eta)$ depends roughly linearly on η. Hence, $\Delta A \approx a \times \eta$

Appendix F. Grand canonical weights as a function of particle number

As shown in *e.g.* Eq. (2) or (40), computation of GCE rates involves a summation over states with different number of particles. To avoid the infinite summation, the crucial question is how many different states are in fact needed. This depends on the population probability or weight of different particle number states.

Here the weights as a function of μ are studied for a graphene sheet. The graphene is modelled using small 4 atom unit cell repeated in the x and y directions. The vacuum along the z-directions is 15Å. The GPAW[159–161] software is used for the DFT calculations. The grid spacing is set to 0.18Å, $16 \times 16 \times 1$ k-point is applied, and exchange-correlation effects are treated using the PBE[162] functional. The system is immersed in a continuum water solvent using the SCMVD model[163] using the standard parameters given in Ref.163. The charged systems are modelled using the homogeneous Poisson-Boltzmann model[3, 20] The weights are computed using the usual definition:

$$p_N = \frac{\exp[-\beta(E_N - \mu N)]}{\sum_N \exp[-\beta(E_N - \mu N)]} \tag{F.1}$$

Charge	$\mu = E_f$	E	$p(\mu = -4.03$ eV)	$p(\mu = -3.06$ eV)
-0.1	-2.46	-37.17	0.0096	0.0536
-0.075	-2.83	-37.11	0.0349	0.1203
-0.05	-3.06	-37.03	0.0988	0.2102
-0.025	-3.53	-36.95	0.2148	0.2825
0	-4.03	-36.86	0.2973	0.2417
0.025	-4.53	-36.75	0.2144	0.1077
0.05	-5.02	-36.63	0.0971	0.0301
0.075	-5.26	-36.50	0.0335	0.0064
0.1	-5.64	-36.36	0.0089	0.0010

Table F.1: Weights for different charge states of graphene as function of μ, the electron chemical potential in eV. E_f is the Fermi-level in eV, E is the total energy, and p are the weights

The results are show in Table F.1. As can be seen the relevant weights for both $\mu_0 = -4.03$ and $\mu = \mu_0 \pm 0.5eV$ are captured by using 9 charge states. By carefully choosing the different charge states will reduce the number needed charge states. Furthermore, larger systems should require less states as these are "closer" to the thermodynamic limit and the probabilities approach a Delta function as system size is increased.

Appendix G. Franck-Condon derivation of the non-adiabatic rate

The Franck-Condon treatment starts from the second-last line of Eq. (36) by noticing that

$$\frac{1}{2\pi\sim}\sum_{m,n} p_{imN} V^2_{N,if} \int dt |\langle nN|mN\rangle|^2 e^{it(E_{imN}-E_{fnN})/\sim} = \frac{V^2_{N,if}}{2\pi} FC(\Delta E)_i \tag{G.1}$$

where $FC(\Delta E)_i$ is the thermalized Franck-Condon factor. In general case, the thermalized Franck-Condon factor can be computed by Fourier transforming it and using generating functions.[164] As shown in Ref. 125 chapter 6,the FC-factor can be written using the spectral density function $J_{fi}(\omega)$ to give

$$
\begin{aligned}
FC(\Delta E)_i &= \frac{1}{2\pi\sim}\exp[G(0)]\int_{-\infty}^{\infty} dt\exp\left[it\Delta E_{fi}^N/\sim + G(t)\right] \\
&\approx \int_{-\infty}^{\infty}\frac{dt}{2\pi\sim}\exp\left[it\frac{\Delta E_{fi}^N-\lambda}{\sim}\right]\exp\left[-\frac{\lambda t^2}{\beta\sim^2}\right] \\
&= \sqrt{\frac{1}{4\pi k_B T\lambda}}\exp\left[-\frac{(\Delta E_{fi}^N+\lambda)^2}{4k_BT\lambda}\right] \qquad \text{(G.2)} \\
&\text{where } G(t) = \int_0^{\infty} d\omega\cos(\omega t)(1+2n(\omega))J_{IF}(\omega) - \sin(\omega t)J_{IF}(\omega) \\
&\approx \int_0^{\infty} d\omega\frac{(\omega t)^2}{\beta\sim\omega}J_{IF}(\omega) - i\int_0^{\infty} d\omega t\omega J_{IF}(\omega)
\end{aligned}
$$

using the high-temperature approximation ($1 + 2n(\omega) \approx 2k_BT >> 1$) and slow-fluctuating Debye solvent assumptions and $\int_0^{\infty} d\omega\omega J_{IF}(\omega) = \lambda/2$ has been used. Hence, if the spectral density not sensitive to the number of electrons, the reorganization energy is independent on the number of electrons in the systems. For practical purposes this is expected to be a good approximation. When the approximate FC factor is introduced, Eq. (G.1) gives the Marcus rate in the GCE.

Appendix H. Decomposition of the reorganization energy to inner- and outer-sphere contributions

The total reorganization energy is often[54, 75, 103, 165] modified differentiate between inner- and outer-sphere contributions. This is achieved by partitioning the surrounding molecules to tightly bound ligands or inner-solvent solvent molecules and the bulk solvent. While this is not necessary in the approach taken in this work, separating the effect the nearby atoms or molecules and the solvent might be useful for a understanding the role of different constituents on the overall reaction. In both computational and theoretical studies this separation occurs naturally if the bulk solvent is presented as a continuum as in the work of Dogonadze *et.al.*[49, 50] for ET and SHS[54] for PCET.

To single out the solvent reorganization energy, a solvent polarization coordinate $\mathcal{Q}$ is introduced. As detailed in Ref. 54 this coordinate introduces a

new parametric dependence to the electron, proton, and vibrational Hamiltonians, wave functions and energies. Here it is shown how an additional solvent coordinate modifies the ET reactions and the PCET kinetics can be treated analogously.

First, a solvent coordinate $\mathcal{Q}$ is introduced. The solvent coordinate is orthogonal to other coordinates which allows writing the wave function as $|imaN\rangle = |iN(q,\mathcal{Q})\rangle\,|mN(\mathcal{Q})\rangle\,|aN\rangle$ where $|aN\rangle$ is the wave function related to solvent polarization. Similarly the energies from Eqs. (42) obtain a parametric dependence on $\mathcal{Q}$. The initial state solvent wave functions are eigenfunctions obtained from

$$[\hat{T}_{\mathcal{Q}} + \epsilon_{mN}]\,|aN\rangle = \mathbb{E}_{aN}\,|aN\rangle \tag{H.1}$$

and similarly for the final state. Above, $\hat{T}_{\mathcal{Q}}$ is the kinetic energy operator for the outer-sphere species. Then the total energy is given by

$$E_{imaN} = \varepsilon_{iN} + \epsilon^{i}_{mN} + \mathbb{E}_{aN} \tag{H.2}$$

and the total coupling between the initial and final states is

$$\begin{aligned} V_{imaN,fnbN} &= \langle fmbN|\hat{V}_N|imaN\rangle \\ &\approx \langle fN|\hat{V}_N|iN\rangle\,\langle nN|mN\rangle_q\,\langle bN|aN\rangle_{\mathcal{Q}} \\ &= V_{if,N}S_{nm,N}\mathcal{S}_{ab,N} \end{aligned} \tag{H.3}$$

Assuming that the outer-sphere free energy related to the solvent reorganization is independent of the particle number allows separating its contribution from the total grand partition function

$$\begin{aligned} \Xi_i &= \sum_{m,a,N} \exp[-\beta(E_{imaN} - \mu N)] \\ &\approx Q_a \sum_{m,N} \exp[-\beta(E_{imN} - \mu N)] = Q_a \Xi_{im} \end{aligned} \tag{H.4}$$

Note that inner-sphere energies and partition function explicitly depend on the particle number. Inserting the last two equations in the golden rule expression yields

$$
\begin{aligned}
k &= \frac{2\pi}{\sim \Xi_i} \sum_{Nabmn} e^{-\beta(\varepsilon_{iN}-\mu N+\beta \mathbb{E}^i_{aN}+\epsilon_{mN})} \Big| \langle Nnvf|\hat{V}_N|iumN\rangle \Big|^2 \delta(E_{imaN} - E_{fnbN}) \\
&\approx \frac{2\pi}{\sim} \sum_N \sum_{m,n} p_{imN} \sum_{a,b} p_{aN} V^2_{if,N} S^2_{nm,N} \mathcal{S}^2_{ab,N} \delta(E_{imaN} - E_{fnbN})
\end{aligned}
\tag{H.5}
$$

where $p_{imN} = \exp[-\beta(\varepsilon_{iN} + \epsilon_{mN} - \mu N)]/\Xi_{im}$ and $p_{aN} = \exp[-\beta \mathbb{E}aN/Q_a]$. As done above, representing the delta function as a Fourier transform allows writing

$$
\begin{aligned}
k &= \sum_N \frac{V^2_{if,N}}{\sim^2} \int dt \left\langle e^{it(\varepsilon_{mN}/\sim} e^{-it(\varepsilon_{nN})/\sim} \right\rangle_q \times \left\langle e^{it(\mathbb{E}_{aN}/\sim} e^{-it(\mathbb{E}_{bN})/\sim} \right\rangle_{\mathcal{Q}} \\
&= \sum_N \frac{V^2_{if,N}}{\sim^2} \int dt G_{mn,N}(t) g_{ab,N}(t)
\end{aligned}
\tag{H.6}
$$

where auxiliary correlation functions $G_{mn,N}(t)$ and $g_{ab,N}(t)$ are introduced providing a connection to the work of SHS[54, 55]. To be specific, $G_{mn,N}(t)$ characterizes the inner-sphere contributions while $g_{ab,N}(t)$ is related to the outer-sphere solvent polarization. Different approximations for the correlation functions presented by SHS in Ref. 54, 55 can be readily used here as well to derive various well-defined limits of the rate equation. For example, assuming that the intra-molecular modes can be neglected leads to Eq.(36) with a/b replacing the m/n indices. Within this assumption and repeating the steps leading to Eq. (40) shows that resulting reorganization energy is the solvent reorganization energy and the inner-sphere interactions contribute only to the reaction energy.

If the intra-sphere contributions cannot be neglected, the rate equations become rather cumbersome in general. However, the case $G_{ab,N}(t) \approx G_{ab}(t)$ *i.e.* that the outer-sphere contribution to rate is independent of the particle number, deserves some attention. For this, the inner- and outer-sphere components are separated by rewriting Eq.(H.5) using a convolution[165]

$$
k = \sum_N p_{iN} \frac{2\pi V^2_{if,N}}{\sim} \int dE f(x) F(\Delta E^N_{fi} - x) \tag{H.7}
$$

with $f(x) = \sum_{mn} p_{mN} S^2_{nm,N} \delta(\epsilon^i_{mN} - \epsilon^i_{nN} + E)$ and $F(E^N_{fi} - x) = \sum_{ab} p_{aN} \mathcal{S}^2_{ab,N} \delta(\mathbb{E}_{aN} - \mathbb{E}_{bN} + \Delta E^N_{fi} - x)$ as shown for single N in Ref.165. $f(x)$ and $F(E^N_{fi} - x)$ represent inner- and outer-sphere contributions to transition probability. Again various forms for both terms can be derived[165]. To retain consistency, a high-temperature approximation for quadratic solvent modes is used. This gives[54, 55, 165]

$$F(E^N_{fi} - x) = \frac{1}{\sim\sqrt{4\pi k_B T \lambda^N_o}} \exp\left[-\frac{(\Delta E^N_{fi} + \lambda^N_o)^2}{4 k_B T \lambda^N_o} \right] \tag{H.8a}$$

$$f(x) = FC(\Delta E - x)_i \tag{H.8b}$$

where $FC(\Delta E - x)_i$ is a modified Franck-Condon factor given in (G.2) and λ^N_o is recognized as the outer-sphere reorganization energy. Making the high-temperature and slow-fluctuating Debye solvent approximations as done in Eq (G.2) allows performing the convolution integral. This yields [165]

$$k = \sum_N p_{iN} \frac{2\pi V^2_{if,N}}{\sim} \frac{1}{\sim\sqrt{4\pi k_B T (\lambda^N_o + \lambda^N_i)}} \exp\left[-\frac{(\Delta E^N_{fi} + \lambda^N_o + \lambda^N_i)^2}{4 k_B T (\lambda^N_o + \lambda^N_i)} \right] \tag{H.9}$$

Finally the assumption that the outer-sphere contributions do not depend on the particle number can be applied to give

$$k = \sum_N p_{iN} \frac{2\pi V^2_{if,N}}{\sim} \frac{1}{\sim\sqrt{4\pi k_B T (\lambda_o + \lambda^N_i)}} \exp\left[-\frac{(\Delta E^N_{fi} + \lambda_o + \lambda^N_i)^2}{4 k_B T (\lambda_o + \lambda^N_i)} \right] \tag{H.10}$$

From this form it can be seen that the total reorganization energy can be separated to a particle number independent solvent contribution λ_o and a reorganization energy of the inner sphere component λ^N_i which depends explicitly on the particle number.

[1] Z. W. Seh, J. Kibsgaard, C. F. Dickens, I. Chorkendorff, J. K. Nørskov, T. F. Jaramillo, Combining theory and experiment in electrocatalysis: Insights into materials design, Science 355 (2017).

[2] L. R. F. Allen J. Bard, Electrochemical Methods: Fundamentals and Applications, 2nd Edition, John Wiley & Sons, 2001.

[3] M. M. Melander, M. J. Kuisma, T. E. K. Christensen, K. Honkala, Grand-canonical approach to density functional theory of electrocatalytic systems: Thermodynamics of solid-liquid interfaces at constant ion and electrode potentials, The Journal of Chemical Physics 150 (2019) 041706.

[4] N. D. Mermin, Thermal properties of the inhomogeneous electron gas, Phys. Rev. 137 (1965) A1441–A1443.

[5] A. Pribram-Jones, S. Pittalis, E. K. U. Gross, K. Burke, Thermal density functional theory in context, in: F. Graziani, M. P. Desjarlais, R. Redmer, S. B. Trickey (Eds.), Frontiers and Challenges in Warm Dense Matter, Springer International Publishing, 2014, pp. 25–60.

[6] R. Evans, The nature of the liquid-vapour interface and other topics in the statistical mechanics of non-uniform, classical fluids, Advances in Physics 28 (1979) 143–200.

[7] T. Kreibich, R. van Leeuwen, E. K. U. Gross, Multicomponent density-functional theory for electrons and nuclei, Phys. Rev. A 78 (2008) 022501.

[8] J. F. Capitani, R. F. Nalewajski, R. G. Parr, Non-oppenheimer density functional theory of molecular systems, The Journal of Chemical Physics 76 (1982) 568–573.

[9] J.-P. H. J.-P. Hansen, Theory of Simple Liquids, 3rd Edition, Academic Press, 2006.

[10] R. Sundararaman, W. A. GoddardIII, T. A. Arias, Grand canonical electronic density-functional theory: Algorithms and applications to electrochemistry, The Journal of Chemical Physics 146 (2017) 114104.

[11] C. D. Taylor, S. A. Wasileski, J.-S. Filhol, M. Neurock, First principles reaction modeling of the electrochemical interface: Consideration and calculation of a tunable surface potential from atomic and electronic structure, Phys. Rev. B 73 (2006) 165402.

[12] J. D. Goodpaster, A. T. Bell, M. Head-Gordon, Identification of possible pathways for c–c bond formation during electrochemical reduction of co2: New theoretical insights from an improved electrochemical model, The Journal of Physical Chemistry Letters 7 (2016) 1471–1477. PMID: 27045040.

[13] M. Otani, O. Sugino, First-principles calculations of charged surfaces and interfaces: A plane-wave nonrepeated slab approach, Phys. Rev. B 73 (2006) 115407.

[14] R. Jinnouchi, A. B. Anderson, Electronic structure calculations of liquid-solid interfaces: Combination of density functional theory and modified poisson-boltzmann theory, Phys. Rev. B 77 (2008) 245417.

[15] E. Skulason, V. Tripkovic, M. E. Bjørketun, S. Gudmundsdóttir, G. Karlberg, J. Rossmeisl, T. Bligaard, H. Jónsson, J. K. Nørskov, Modeling the electrochemical hydrogen oxidation and evolution reactions on the basis of density functional theory calculations, The Journal of Physical Chemistry C 114 (2010) 18182–18197.

[16] K. Letchworth-Weaver, T. A. Arias, Joint density functional theory of the electrode-electrolyte interface: Application to fixed electrode potentials, interfacial capacitances, and potentials of zero charge, Phys. Rev. B 86 (2012) 075140.

[17] Y.-H. Fang, Z.-P. Liu, Mechanism and tafel lines of electro-oxidation of water to oxygen on ruo2(110), Journal of the American Chemical Society 132 (2010) 18214–18222. PMID: 21133410.

[18] E. Skulason, G. S. Karlberg, J. Rossmeisl, T. Bligaard, J. Greeley, H. Jónsson, J. K. Nørskov, Density functional theory calculations for the hydrogen evolution reaction in an electrochemical double layer on the pt(111) electrode, Phys. Chem. Chem. Phys. 9 (2007) 3241–3250.

[19] K. Chan, J. K. Nørskov, Electrochemical barriers made simple, The Journal of Physical Chemistry Letters 6 (2015) 2663–2668. PMID: 26266844.

[20] G. Kastlunger, P. Lindgren, A. A. Peterson, Controlled-potential simulation of elementary electrochemical reactions: Proton discharge on metal surfaces, The Journal of Physical Chemistry C 122 (2018) 12771–12781.

[21] A. Ignaczak, R. Nazmutdinov, A. Goduljan, L. M. de Campos Pinto, F. Juarez, P. Quaino, G. Belletti, E. Santos, W. Schmickler, Oxygen reduction in alkaline media—a discussion, Electrocatalysis 8 (2017) 554–564.

[22] Z. K. Goldsmith, Y. C. Lam, A. V. Soudackov, S. Hammes-Schiffer, Proton discharge on a gold electrode from triethylammonium in acetonitrile: Theoretical modeling of potential-dependent kinetic isotope effects, Journal of the American Chemical Society 141 (2019) 1084–1090.

[23] K. Sakaushi, A. Lyalin, T. Taketsugu, K. Uosaki, Quantum-to-classical transition of proton transfer in potential-induced dioxygen reduction, Phys. Rev. Lett. 121 (2018) 236001.

[24] A. Ignaczak, R. Nazmutdinov, A. Goduljan, L. M. de Campos Pinto, F. Juarez, P. Quaino, E. Santos, W. Schmickler, A scenario for oxygen reduction in alkaline media, Nano Energy 29 (2016) 362 – 368. Electrocatalysis.

[25] D. Malko, A. Kucernak, Kinetic isotope effect in the oxygen reduction reaction (orr) over fe-n/c catalysts under acidic and alkaline conditions, Electrochemistry Communications 83 (2017) 67 – 71.

[26] E. C. M. Tse, J. A. Varnell, T. T. H. Hoang, A. A. Gewirth, Elucidating proton involvement in the rate-determining step for pt/pd-based and non-precious-metal oxygen reduction reaction catalysts using the kinetic isotope effect, The Journal of Physical Chemistry Letters 7 (2016) 3542–3547. PMID: 27550191.

[27] V. J. Bukas, H. W. Kim, R. Sengpiel, K. Knudsen, J. Voss, B. D. McCloskey, A. C. Luntz, Combining experiment and theory to unravel the

mechanism of two-electron oxygen reduction at a selective and active co-catalyst, ACS Catalysis 8 (2018) 11940–11951.

[28] H. W. Kim, M. B. Ross, N. Kornienko, L. Zhang, J. Guo, P. Yang, B. D. McCloskey, Efficient hydrogen peroxide generation using reduced graphene oxide-based oxygen reduction electrocatalysts, Nature Catalysis 1 (2018) 282–290.

[29] A. J. Gottle, M. T. M. Koper, Proton-coupled electron transfer in the electrocatalysis of co2 reduction: prediction of sequential vs. concerted pathways using dft, Chem. Sci. 8 (2017) 458–465.

[30] S. Verma, Y. Hamasaki, C. Kim, W. Huang, S. Lu, H.-R. M. Jhong, A. A. Gewirth, T. Fujigaya, N. Nakashima, P. J. A. Kenis, Insights into the low overpotential electroreduction of co2 to co on a supported gold catalyst in an alkaline flow electrolyzer, ACS Energy Letters 3 (2018) 193–198.

[31] M. T. M. Koper, Theory of multiple proton-electron transfer reactions and its implications for electrocatalysis, Chem. Sci. 4 (2013) 2710–2723.

[32] S. Hammes-Schiffer, A. A. Stuchebrukhov, Theory of coupled electron and proton transfer reactions, Chemical Reviews 110 (2010) 6939–6960. PMID: 21049940.

[33] H. Xiao, T. Cheng, W. A. Goddard, Atomistic mechanisms underlying selectivities in c1 and c2 products from electrochemical reduction of co on cu(111), Journal of the American Chemical Society 139 (2017) 130–136. PMID: 28001061.

[34] H. Xiao, T. Cheng, W. A. Goddard, R. Sundararaman, Mechanistic explanation of the ph dependence and onset potentials for hydrocarbon products from electrochemical reduction of co on cu (111), Journal of the American Chemical Society 138 (2016) 483–486. PMID: 26716884.

[35] H. Zhang, W. A. Goddard, Q. Lu, M.-J. Cheng, The importance of grand-canonical quantum mechanical methods to describe the effect of electrode potential on the stability of intermediates involved in both electrochemical co2 reduction and hydrogen evolution, Phys. Chem. Chem. Phys. 20 (2018) 2549–2557.

[36] Y. Huang, R. J. Nielsen, W. A. Goddard, The reaction mechanism for the hydrogen evolution reaction on the basal plane sulfur vacancy site of mos2 using grand canonical potential kinetics, Journal of the American Chemical Society 0 (0) null.

[37] N. Holmberg, K. Laasonen, Ab initio electrochemistry: Exploring the hydrogen evolution reaction on carbon nanotubes, The Journal of Physical Chemistry C 119 (2015) 16166–16178.

[38] S. A. Akhade, N. J. Bernstein, M. R. Esopi, M. J. Regula, M. J. Janik, A simple method to approximate electrode potential-dependent activation energies using density functional theory, Catalysis Today 288 (2017) 63 – 73. Electrochemical Reduction of Carbon Dioxide by heterogenous and homogeneous catalysts: Experiment and Theory.

[39] V. Tripkovic, M. E. Björketun, E. Skúlason, J. Rossmeisl, Standard hydrogen electrode and potential of zero charge in density functional calculations, Phys. Rev. B 84 (2011) 115452.

[40] H.-J. Chun, V. Apaja, A. Clayborne, K. Honkala, J. Greeley, Atomistic insights into nitrogen-cycle electrochemistry: A combined dft and kinetic monte carlo analysis of no electrochemical reduction on pt(100), ACS Catalysis 7 (2017) 3869–3882.

[41] D. Bohra, I. Ledezma-Yanez, G. Li, W. de Jong, E. A. Pidko, W. A. Smith, Lateral adsorbate interactions inhibit hcoo while promoting co selectivity for co2 electrocatalysis on silver, Angewandte Chemie 131 (2019) 1359–1363.

[42] A. Ignaczak, R. Nazmutdinov, A. Goduljan, L. M. de Campos Pinto, F. Juarez, P. Quaino, G. Belletti, E. Santos, W. Schmickler, Oxygen reduction in alkaline media—a discussion, Electrocatalysis 8 (2017) 554–564.

[43] A. Goduljan, L. M. de Campos Pinto, F. Juarez, E. Santos, W. Schmickler, Oxygen reduction on ag(100) in alkaline solutions: A theoretical study, ChemPhysChem 17 (2016) 500–505.

[44] W. Schmickler, E. Santos, M. Bronshtein, R. Nazmutdinov, Adiabatic electron-transfer reactions on semiconducting electrodes, ChemPhysChem 18 (2017) 111–116.

[45] C. Venkataraman, A. V. Soudackov, S. Hammes-Schiffer, Theoretical formulation of nonadiabatic electrochemical proton-coupled electron transfer at metalsolution interfaces, The Journal of Physical Chemistry C 112 (2008) 12386–12397.

[46] I. Navrotskaya, A. V. Soudackov, S. Hammes-Schiffer, Model system-bath hamiltonian and nonadiabatic rate constants for proton-coupled electron transfer at electrode-solution interfaces, The Journal of Chemical Physics 128 (2008) 244712.

[47] S. Ghosh, A. V. Soudackov, S. Hammes-Schiffer, Electrochemical electron transfer and proton-coupled electron transfer: Effects of double layer and ionic environment on solvent reorganization energies, Journal of Chemical Theory and Computation 12 (2016) 2917–2925. PMID: 27111050.

[48] S. Ghosh, S. Horvath, A. V. Soudackov, S. Hammes-Schiffer, Electrochemical solvent reorganization energies in the framework of the polarizable continuum model, Journal of Chemical Theory and Computation 10 (2014) 2091–2102. PMID: 26580536.

[49] R. Dogonadze, A. Kuznetsov, Theory of charge transfer kinetics at solid-polar liquid interfaces, Progress in Surface Science 6 (1975) 1 – 41.

[50] R. Dogonadze, 3. theory of molecular electrode kinetics, in: N. Hush (Ed.), Reactions of Molecules at Electrodes, Wiley-Intersciences, 1971, pp. 135–228.

[51] W. Schmickler, A theory of adiabatic electron-transfer reactions, Journal of Electroanalytical Chemistry and Interfacial Electrochemistry 204 (1986) 31 – 43.

[52] W. Schmickler, Adiabatic and non-adiabatic electrochemical electron transfer in terms of green's function theory, Russian Journal of Electrochemistry 53 (2017) 1182–1188.

[53] A. Soudackov, S. Hammes-Schiffer, Multistate continuum theory for multiple charge transfer reactions in solution, The Journal of Chemical Physics 111 (1999) 4672–4687.

[54] A. Soudackov, S. Hammes-Schiffer, Derivation of rate expressions for nonadiabatic proton-coupled electron transfer reactions in solution, The Journal of Chemical Physics 113 (2000) 2385–2396.

[55] A. Soudackov, E. Hatcher, S. Hammes-Schiffer, Quantum and dynamical effects of proton donor-acceptor vibrational motion in nonadiabatic proton-coupled electron transfer reactions, The Journal of Chemical Physics 122 (2005) 014505.

[56] D. Borgis, J. T. Hynes, Dynamical theory of proton tunneling transfer rates in solution: general formulation, Chemical Physics 170 (1993) 315 – 346.

[57] D. Borgis, J. T. Hynes, Curve crossing formulation for proton transfer reactions in solution, The Journal of Physical Chemistry 100 (1996) 1118–1128.

[58] R. I. Cukier, Proton-coupled electron transfer reactions: evaluation of rate constants, The Journal of Physical Chemistry 100 (1996) 15428–15443.

[59] N. Ananth, T. F. M. III, Flux-correlation approach to characterizing reaction pathways in quantum systems: a study of condensed-phase proton-coupled electron transfer, Molecular Physics 110 (2012) 1009–1015.

[60] J. S. Kretchmer, T. F. Miller, Direct simulation of proton-coupled electron transfer across multiple regimes, The Journal of Chemical Physics 138 (2013) 134109.

[61] W. H. Miller, Quantum mechanical transition state theory and a new semiclassical model for reaction rate constants, The Journal of Chemical Physics 61 (1974) 1823–1834.

[62] W. H. Miller, S. D. Schwartz, J. W. Tromp, Quantum mechanical rate constants for bimolecular reactions, The Journal of Chemical Physics 79 (1983) 4889–4898.

[63] W. H. Miller, Direct and correct calculation of canonical and microcanonical rate constants for chemical reactions, The Journal of Physical Chemistry A 102 (1998) 793–806.

[64] I. R. Craig, D. E. Manolopoulos, A refined ring polymer molecular dynamics theory of chemical reaction rates, The Journal of Chemical Physics 123 (2005) 034102.

[65] T. J. H. Hele, S. C. Althorpe, An alternative derivation of ring-polymer molecular dynamics transition-state theory, The Journal of Chemical Physics 144 (2016) 174107.

[66] S. C. Althorpe, T. J. H. Hele, Derivation of a true ($t \to 0+$) quantum transition-state theory. ii. recovery of the exact quantum rate in the absence of recrossing, The Journal of Chemical Physics 139 (2013) 084115.

[67] J. O. Richardson, S. C. Althorpe, Ring-polymer molecular dynamics rate-theory in the deep-tunneling regime: Connection with semiclassical instanton theory, The Journal of Chemical Physics 131 (2009) 214106.

[68] G. Mills, G. Schenter, D. Makarov, H. Jónsson, Generalized path integral based quantum transition state theory, Chemical Physics Letters 278 (1997) 91 – 96.

[69] W. H. Miller, Semiclassical limit of quantum mechanical transition state theory for nonseparable systems, The Journal of Chemical Physics 62 (1975) 1899–1906.

[70] R. Hernandez, W. H. Miller, Semiclassical transition state theory. a new perspective, Chemical Physics Letters 214 (1993) 129 – 136.

[71] W. H. Miller, R. Hernandez, N. C. Handy, D. Jayatilaka, A. Willetts, Ab initio calculation of anharmonic constants for a transition state, with application to semiclassical transition state tunneling probabilities, Chemical Physics Letters 172 (1990) 62 – 68.

[72] J. O. Richardson, R. Bauer, M. Thoss, Semiclassical green's functions and an instanton formulation of electron-transfer rates in the nonadiabatic limit, The Journal of Chemical Physics 143 (2015) 134115.

[73] P. Shushkov, On the connection of semiclassical instanton theory with marcus theory for electron transfer in solution, The Journal of Chemical Physics 138 (2013) 224102.

[74] J. Mattiat, J. O. Richardson, Effects of tunnelling and asymmetry for system-bath models of electron transfer, The Journal of Chemical Physics 148 (2018) 102311.

[75] R. A. Marcus, On the theory of electron transfer reactions. vi. unified treatment for homogeneous and electrode reactions, The Journal of Chemical Physics 43 (1965) 679–701.

[76] R. v. L. Gianluca Stefanucci, Nonequilibrium Many-Body Theory pf Quantum Systems: A Modern Introduction, Cambridge University Press, pp. 81–124.

[77] A. Agarwal, J. Zhu, C. Hartmann, H. Wang, L. D. Site, Molecular dynamics in a grand ensemble: Bergmannlebowitz model and adaptive resolution simulation, New Journal of Physics 17 (2015) 083042.

[78] M. Tuckerman, Statistical Mechanics: Theory and Molecular Simulations, Oxford University Press, 2010.

[79] M. H. Peters, An extended liouville equation for variable particle number systems, eprint arXiv:physics/9809039 (1998).

[80] R. P. Feynman, Space-time approach to non-relativistic quantum mechanics, Rev. Mod. Phys. 20 (1948) 367–387.

[81] S. Habershon, D. E. Manolopoulos, T. E. Markland, T. F. Miller, Ring-polymer molecular dynamics: Quantum effects in chemical dynamics from classical trajectories in an extended phase space, Annual Review of Physical Chemistry 64 (2013) 387–413. PMID: 23298242.

[82] J. O. Richardson, M. Thoss, Non-oscillatory flux correlation functions for efficient nonadiabatic rate theory, The Journal of Chemical Physics 141 (2014) 074106.

[83] J. O. Richardson, M. Thoss, Communication: Nonadiabatic ring-polymer molecular dynamics, The Journal of Chemical Physics 139 (2013) 031102.

[84] A. Agarwal, L. Delle Site, Path integral molecular dynamics within the grand canonical-like adaptive resolution technique: Simulation of liquid water, The Journal of Chemical Physics 143 (2015) 094102.

[85] J. O. Richardson, Ring-polymer instanton theory, International Reviews in Physical Chemistry 37 (2018) 171–216.

[86] N. E. Henriksen, F. Y. Hansen, Transition-state theory and dynamical corrections, Phys. Chem. Chem. Phys. 4 (2002) 5995–6000.

[87] D. Chandler, Statistical mechanics of isomerization dynamics in liquids and the transition state approximation, The Journal of Chemical Physics 68 (1978) 2959–2970.

[88] G. Henkelman, B. P. Uberuaga, H. Jónsson, A climbing image nudged elastic band method for finding saddle points and minimum energy paths, The Journal of Chemical Physics 113 (2000) 9901–9904.

[89] A. Warshel, R. M. Weiss, An empirical valence bond approach for comparing reactions in solutions and in enzymes, Journal of the American Chemical Society 102 (1980) 6218–6226.

[90] S. C. L. Kamerlin, A. Warshel, The empirical valence bond model: theory and applications, Wiley Interdisciplinary Reviews: Computational Molecular Science 1 (2011) 30–45.

[91] U. W. Schmitt, G. A. Voth, Multistate empirical valence bond model for proton transport in water, The Journal of Physical Chemistry B 102 (1998) 5547–5551.

[92] R. Vuilleumier, D. Borgis, Quantum dynamics of an excess proton in water using an extended empirical valence-bond hamiltonian, The Journal of Physical Chemistry B 102 (1998) 4261–4264.

[93] J. R. Reimers, L. K. McKemmish, R. H. McKenzie, N. S. Hush, Non-adiabatic effects in thermochemistry, spectroscopy and kinetics: the general importance of all three born-oppenheimer breakdown corrections, Phys. Chem. Chem. Phys. 17 (2015) 24641–24665.

[94] L. K. McKemmish, R. H. McKenzie, N. S. Hush, J. R. Reimers, Electron-vibration entanglement in the born-oppenheimer description of chemical reactions and spectroscopy, Phys. Chem. Chem. Phys. 17 (2015) 24666–24682.

[95] Q. Wu, T. Van Voorhis, Direct optimization method to study constrained systems within density-functional theory, Phys. Rev. A 72 (2005) 024502.

[96] Q. Wu, T. Van Voorhis, Extracting electron transfer coupling elements from constrained density functional theory, J. Chem. Phys. 125 (2006) 164105.

[97] B. Kaduk, T. Kowalczyk, T. V. Voorhis, Constrained density functional theory, Chem. Rev. 112 (2012) 321–370.

[98] L. Zusman, Outer-sphere electron transfer in polar solvents, Chemical Physics 49 (1980) 295 – 304.

[99] A. Warshel, Dynamics of reactions in polar solvents. semiclassical trajectory studies of electron-transfer and proton-transfer reactions, The Journal of Physical Chemistry 86 (1982) 2218–2224.

[100] J. Blumberger, Recent advances in the theory and molecular simulation of biological electron transfer reactions, Chemical Reviews 115 (2015) 11191–11238. PMID: 26485093.

[101] A. Nitzan, Chemical Dynamics in Condendsed Phases: Relaxation, Transfer, and Reactions in Condensed Molecular Systems, Oxford University Press, 2006.

[102] R. R. Dogonadze, A. M. Kuznetsov, A. A. Chernenko, Theory of homogeneous and heterogeneous electronic processes in liquids, Russ. Chem. Rev. 34 (1965) 759.

[103] S. K. J.O.M Bockris, Quantum Electrochemistry, Plenum Press, 1979.

[104] R. W. Zwanzig, High-temperature equation of state by a perturbation method. i. nonpolar gases, The Journal of Chemical Physics 22 (1954) 1420–1426.

[105] M. Tachiya, Relation between the electron-transfer rate and the free energy change of reaction, The Journal of Physical Chemistry 93 (1989) 7050–7052.

[106] Y. Tateyama, J. Blumberger, M. Sprik, I. Tavernelli, Density-functional molecular-dynamics study of the redox reactions of two anionic, aqueous transition-metal complexes, The Journal of Chemical Physics 122 (2005) 234505.

[107] R. Vuilleumier, K. A. Tay, G. Jeanmairet, D. Borgis, A. Boutin, Extension of marcus picture for electron transfer reactions with large solvation changes, Journal of the American Chemical Society 134 (2012) 2067–2074. PMID: 22148250.

[108] D. A. Rose, I. Benjamin, Molecular dynamics of adiabatic and nonadiabatic electron transfer at the metalwater interface, The Journal of Chemical Physics 100 (1994) 3545–3555.

[109] H.-. Zhou, A. Szabo, Microscopic formulation of marcus theory of electron transfer, The Journal of Chemical Physics 103 (1995) 3481–3494.

[110] G. King, A. Warshel, Investigation of the free energy functions for electron transfer reactions, The Journal of Chemical Physics 93 (1990) 8682–8692.

[111] A. Warshel, J. K. Hwang, J. Åqvist, Computer simulations of enzymatic reactions: examination of linear free-energy relationships and quantum-mechanical corrections in the initial proton-transfer step of carbonic anhydrase, Faraday Discuss. 93 (1992) 225–238.

[112] E. Rosta, A. Warshel, Origin of linear free energy relationships: Exploring the nature of the off-diagonal coupling elements in sn2 reactions, Journal of Chemical Theory and Computation 8 (2012) 3574–3585. PMID: 23329895.

[113] S. Trasatti, The absolute electrode potential the end of the story, Electrochimica Acta 35 (1990) 269 – 271.

[114] S. Trasatti, The absolute electrode potential: an explanatory note (recommendations 1986), Journal of Electroanalytical Chemistry and Interfacial Electrochemistry 209 (1986) 417 – 428.

[115] S. Fletcher, The theory of electron transfer, Journal of Solid State Electrochemistry 14 (2010) 705–739.

[116] S. Fletcher, Tafel slopes from first principles, Journal of Solid State Electrochemistry 13 (2009) 537–549.

[117] R. Parsons, General equations for the kinetics of electrode processes, Trans. Faraday Soc. 47 (1951) 1332–1344.

[118] J. K. Nørskov, J. Rossmeisl, A. Logadottir, L. Lindqvist, J. R. Kitchin, T. Bligaard, H. Jónsson, Origin of the overpotential for oxygen reduction at a fuel-cell cathode, The Journal of Physical Chemistry B 108 (2004) 17886–17892.

[119] N. G. Hörmann, O. Andreussi, N. Marzari, Grand canonical simulations of electrochemical interfaces in implicit solvation models, The Journal of Chemical Physics 150 (2019) 041730.

[120] C. E. D. CHIDSEY, Free energy and temperature dependence of electron transfer at the metal-electrolyte interface, Science 251 (1991) 919–922.

[121] X. Sun, E. Geva, Equilibrium fermi's golden rule charge transfer rate constants in the condensed phase: The linearized semiclassical method vs classical marcus theory, The Journal of Physical Chemistry A 120 (2016) 2976–2990. PMID: 26452042.

[122] Y. Georgievskii, C.-P. Hsu, R. A. Marcus, Linear response in theory of electron transfer reactions as an alternative to the molecular harmonic oscillator model, The Journal of Chemical Physics 110 (1999) 5307–5317.

[123] R. Kubo, Generalized Cumulant Expansion Method, Journal of the Physical Society of Japan 17 (1962) 1100–1120.

[124] D. C. Borgis, S. Lee, J. T. Hynes, A dynamical theory of nonadiabatic proton and hydrogen atom transfer reaction rates in solution, Chemical Physics Letters 162 (1989) 19 – 26.

[125] V. May, O. Kühn, Charge and Energy Transfer Dynamics in Molecular Systems, volume 3rd, WILEY-VCH Verlag GmbH & Co. KGaA, Weinheim, 2011.

[126] S. Hammes-Schiffer, Proton-coupled electron transfer: classification scheme and guide to theoretical methods, Energy Environ. Sci. 5 (2012) 7696–7703.

[127] S. Hammes-Schiffer, E. Hatcher, H. Ishikita, J. H. Skone, A. V. Soudackov, Theoretical studies of proton-coupled electron transfer: Models and concepts relevant to bioenergetics, Coordination Chemistry Reviews 252 (2008) 384 – 394. The Role of Manganese in Photosystem II.

[128] Y. Georgievskii, A. A. Stuchebrukhov, Concerted electron and proton transfer: Transition from nonadiabatic to adiabatic proton tunneling, The Journal of Chemical Physics 113 (2000) 10438–10450.

[129] J. H. Skone, A. V. Soudackov, S. Hammes-Schiffer, Calculation of vibronic couplings for phenoxyl/phenol and benzyl/toluene self-exchange reactions: implications for proton-coupled electron transfer mechanisms, Journal of the American Chemical Society 128 (2006) 16655–16663. PMID: 17177415.

[130] H. Park, N. Kumar, M. Melander, T. Vegge, J. M. Garcia Lastra, D. J. Siegel, Adiabatic and nonadiabatic charge transport in li–s batteries, Chemistry of Materials 30 (2018) 915–928.

[131] T. Ikeshoji, M. Otani, Toward full simulation of the electrochemical oxygen reduction reaction on pt using first-principles and kinetic calculations, Phys. Chem. Chem. Phys. 19 (2017) 4447–4453.

[132] M. Van den Bossche, E. Skulason, C. Rose-Petruck, H. Jónsson, Assessment of constant-potential implicit solvation calculations of electrochemical energy barriers for h2 evolution on pt, The Journal of Physical Chemistry C 0 (0) null.

[133] Z.-F. Huang, J. Wang, Y. Peng, C.-Y. Jung, A. Fisher, X. Wang, Design of efficient bifunctional oxygen reduction/evolution electrocatalyst: Recent advances and perspectives, Advanced Energy Materials 7 (2017) 1700544–n/a. 1700544.

[134] S. Back, Y. Jung, Importance of ligand effects breaking the scaling relation for coreshell oxygen reduction catalysts, ChemCatChem 9 (2017) 3173–3179.

[135] A. Kulkarni, S. Siahrostami, A. Patel, J. K. Nørskov, Understanding catalytic activity trends in the oxygen reduction reaction, Chemical Reviews 0 (0) null. PMID: 29405702.

[136] Z.-D. He, Y.-X. Chen, E. Santos, W. Schmickler, The pre-exponential factor in electrochemistry, Angewandte Chemie International Edition 57 (2018) 7948–7956.

[137] A. M. Souza, I. Rungger, C. D. Pemmaraju, U. Schwingenschloegl, S. Sanvito, Constrained-dft method for accurate energy-level alignment of metal/molecule interfaces, Phys. Rev. B 88 (2013) 165112.

[138] Q. Wu, B. Kaduk, T. Van Voorhis, Constrained density functional theory based configuration interaction improves the prediction of reaction barrier heights, J. Chem. Phys. 130 (2009) 034109.

[139] J. Řezáč, B. Lévy, I. Demachy, A. de la Lande, Robust and efficient constrained dft molecular dynamics approach for biochemical modeling, J. Chem. Theory Comput. 8 (2012) 418–427.

[140] P. Ramos, M. Pavanello, Constrained subsystem density functional theory, Phys. Chem. Chem. Phys. 18 (2016) 21172–21178.

[141] H. Oberhofer, J. Blumberger, Charge constrained density functional molecular dynamics for simulation of condensed phase electron transfer reactions, J. Chem. Phys. 131 (2009) 064101.

[142] H. Oberhofer, J. Blumberger, Electronic coupling matrix elements from charge constrained density functional theory calculations using a plane wave basis set, J. Chem. Phys. 133 (2010) 244105.

[143] P. Ghosh, R. Gebauer, Computational approaches to charge transfer excitations in a zinc tetraphenylporphyrin and c70 complex, J. Chem. Phys. 132 (2010) 104102.

[144] A. M. P. Sena, T. Miyazaki, D. R. Bowler, Linear scaling constrained density functional theory in conquest, J. Chem. Theory Comput. 7 (2011) 884–889.

[145] L. E. Ratcliff, L. Grisanti, L. Genovese, T. Deutsch, T. Neumann, D. Danilov, W. Wenzel, D. Beljonne, J. Cornil, Toward fast and

accurate evaluation of charge on-site energies and transfer integrals in supramolecular architectures using linear constrained density functional theory (cdft)-based methods, J. Chem. Theory Comput. 11 (2015) 2077–2086.

[146] M. Melander, E. O. Jónsson, J. J. Mortensen, T. Vegge, J. M. García Lastra, Implementation of constrained dft for computing charge transfer rates within the projector augmented wave method, Journal of Chemical Theory and Computation 12 (2016) 5367–5378. PMID: 27749068.

[147] N. Holmberg, K. Laasonen, Efficient constrained density functional theory implementation for simulation of condensed phase electron transfer reactions, Journal of Chemical Theory and Computation 13 (2017) 587–601. PMID: 28009515.

[148] R. Memming, Semiconductor Electrochemistry, WILEY-VCH Verlag GmbH, 2001.

[149] A. K. Mishra, D. H. Waldeck, Comparison of the density of states (dos) and potential energy curve (pec) models for the electrochemical rate constant, The Journal of Physical Chemistry C 115 (2011) 20662–20673.

[150] N. Marzari, A. A. Mostofi, J. R. Yates, I. Souza, D. Vanderbilt, Maximally localized wannier functions: Theory and applications, Rev. Mod. Phys. 84 (2012) 1419–1475.

[151] S. Lehtola, H. Jónsson, Unitary optimization of localized molecular orbitals, Journal of Chemical Theory and Computation 9 (2013) 5365–5372. PMID: 26592274.

[152] G. Knizia, Intrinsic atomic orbitals: An unbiased bridge between quantum theory and chemical concepts, Journal of Chemical Theory and Computation 9 (2013) 4834–4843. PMID: 26583402.

[153] C. Edmiston, K. Ruedenberg, Localized atomic and molecular orbitals, Rev. Mod. Phys. 35 (1963) 457–464.

[154] K. S. Thygesen, L. B. Hansen, K. W. Jacobsen, Partly occupied wannier functions: Construction and applications, Phys. Rev. B 72 (2005) 125119.

[155] F. Gajdos, S. Valner, F. Hoffmann, J. Spencer, M. Breuer, A. Kubas, M. Dupuis, J. Blumberger, Ultrafast estimation of electronic couplings for electron transfer between -conjugated organic molecules, Journal of Chemical Theory and Computation 10 (2014) 4653–4660. PMID: 26588156.

[156] H. Oberhofer, J. Blumberger, Revisiting electronic couplings and incoherent hopping models for electron transport in crystalline c60 at ambient temperatures, Phys. Chem. Chem. Phys. 14 (2012) 13846–13852.

[157] G. Jeanmairet, B. Rotenberg, M. Levesque, D. Borgis, M. Salanne, A molecular density functional theory approach to electron transfer reactions, Chem. Sci. 10 (2019) 2130–2143.

[158] F. O. Raineri, H. L. Friedman, Solvent Control of Electron Transfer Reactions, John Wiley & Sons, Ltd, pp. 81–189.

[159] J. J. Mortensen, L. B. Hansen, K. W. Jacobsen, Real-space grid implementation of the projector augmented wave method, Phys. Rev. B 71 (2005) 035109.

[160] J. Enkovaara, C. Rostgaard, J. J. Mortensen, J. Chen, M. Dułak, L. Ferrighi, J. Gavnholt, C. Glinsvad, V. Haikola, H. A. Hansen, H. H. Kristoffersen, M. Kuisma, A. H. Larsen, L. Lehtovaara, M. Ljungberg, O. Lopez-Acevedo, P. G. Moses, J. Ojanen, T. Olsen, V. Petzold, N. A. Romero, J. Stausholm-Møller, M. Strange, G. A. Tritsaris, M. Vanin, M. Walter, B. Hammer, H. Häkkinen, G. K. H. Madsen, R. M. Nieminen, J. K. Nørskov, M. Puska, T. T. Rantala, J. Schiøtz, K. S. Thygesen, K. W. Jacobsen, Electronic structure calculations with gpaw: a real-space implementation of the projector augmented-wave method, J. Phys. Condens. Matter 22 (2010) 253202.

[161] A. H. Larsen, J. J. Mortensen, J. Blomqvist, I. E. Castelli, R. Christensen, M. Dułak, J. Friis, M. N. Groves, B. Hammer, C. Hargus, E. D. Hermes, P. C. Jennings, P. B. Jensen, J. Kermode, J. R. Kitchin,

E. L. Kolsbjerg, J. Kubal, K. Kaasbjerg, S. Lysgaard, J. B. Maronsson, T. Maxson, T. Olsen, L. Pastewka, A. Peterson, C. Rostgaard, J. Schiøtz, O. Schtt, M. Strange, K. S. Thygesen, T. Vegge, L. Vilhelmsen, M. Walter, Z. Zeng, K. W. Jacobsen, The atomic simulation environment—a python library for working with atoms, Journal of Physics: Condensed Matter 29 (2017) 273002.

[162] J. P. Perdew, K. Burke, M. Ernzerhof, Generalized gradient approximation made simple, Phys. Rev. Lett. 77 (1996) 3865–3868.

[163] A. Held, M. Walter, Simplified continuum solvent model with a smooth cavity based on volumetric data, The Journal of Chemical Physics 141 (2014) 174108.

[164] R. Englman, J. Jortner, The energy gap law for radiationless transitions in large molecules, Molecular Physics 18 (1970) 145–164.

[165] N. R. Kestner, J. Logan, J. Jortner, Thermal electron transfer reactions in polar solvents, The Journal of Physical Chemistry 78 (1974) 2148–2166.